Magee Womens Research Institute and Foundation

Annual Progress Report: 2009 Formula Grant

Reporting Period

July 1, 2010 – December 31, 2010

Formula Grant Overview

The Magee Womens Research Institute and Foundation received $1,541,095 in formula funds for the grant award period January 1, 2010, through December 31, 2010. Accomplishments for the reporting period are described below.

Research Project 1: Project Title and Purpose

Refinement of the Appropriate Animal Model for Respiratory Infection with Influenza in Pregnancy - The purpose of the project is to develop and test a ferret model for respiratory challenge with influenza virus infection during pregnancy. This is critical given the disproportionate morbidity and mortality seen among pregnant women during previous influenza pandemics, seasonal epidemics and the current novel 2009 H1N1 influenza pandemic. Development of a pregnant animal model for respiratory challenge will also allow for future investigations to delineate more effectively the susceptibility to infection noted among pregnant women and their immunological response mechanisms. In addition, with the growing threat of bioterrorism and the fact that most category a bioterror agents would be targeted for inhalational spread, development of pregnant animal models allows for ongoing countermeasures' research against these agents in this unique population.

Duration of Project

1/1/2010 - 12/31/2010

Project Overview

1. Further develop and refine a model of collaboration and infrastructure that will allow for ongoing investigation of susceptibility, immunological response and countermeasures to emerging and threatening infectious diseases among pregnant animals.
2. To demonstrate and compare the disease course of aerosolized novel 2009 H1N1 in both a late gestation pregnant and non-pregnant ferret model of influenza infection.
3. To evaluate and compare the pathogenesis and immune response elicited by aerosolized novel 2009 H1N1 in both late gestation pregnant and non-pregnant ferrets.

We will begin by examining aerosol characteristics of novel 2009 H1N1 influenza at 3 dilutions in an empty aerosol chamber starting at 10^8/ml and decreasing ten-fold. Four aerosols per dilution (12 aerosols) will be used in a whole-body exposure box and will then be repeated once

for validation. Subsequent determinations of viral concentration in the nebulizer and aerosol by Tissue Culture ID50 (TCID50) will be undertaken. After these quality and quantity control measures, challenge experiments will then be undertaken. Ferrets obtained from Marshall Pet Products will be used for the experiments. In order to determine the Infective Dose of 2009 H1N1 that establishes infection in 50% of ferrets (IC_{50}), aerosol challenges with 3 doses in a whole-body chamber at doses expected to bracket the IC_{50} will be performed upon 3 groups of four. Fifty percent of ferrets will be pregnant and 50% non-pregnant. Challenges will be performed on or about day 33 of a 42 day gestation, approximating 3rd trimester exposure. All ferrets will be followed for 10-14 days after exposure to document clinical disease course and to quantify upper respiratory tract viral load (PCR). Ferrets that become moribund will be promptly euthanized and necropsied; blood and tissue samples will be taken for analysis. Subsequently, challenges using the determined IC_{50} from the above aim will be performed among a second group of ferrets with four in each group (pregnant and non-pregnant, total N=8). The first group will undergo a sham challenge for control purposes. The next 3 groups will be challenged and then euthanized at days 2, 4 and 7 post-challenge. Pre-euthanization analysis will include: Viral load, Hemagluttin and microneutralization antibody titers, and potentially microarray technologies pending funding specifics. Post-euthanization analysis will include both pathologic and viral load quantification of tissue specimens, including the fetal compartment.

Principal Investigator

Richard H. Beigi, MD, MSc
Assistant Professor of Reproductive Sciences
Magee-Womens Hospital of UPMC
300 Halket Street
Department of OB/GYN/RS
Pittsburgh, PA 15213

Other Participating Researchers

Kelly Stefano-Cole, PhD, Doug Reed, PhD, Amy Hartman, PhD - employed by University of Pittsburgh, Center for Vaccine Research

Expected Research Outcomes and Benefits

We expect to develop a model for exposing ferrets to respiratory challenge with novel 2009 H1N1 influenza. This will allow for comparisons between pregnant and non-pregnant ferrets which is a unique component of this project. The understanding of pregnant women's increased severity of illness from influenza is not completely understood and was readily apparent during the current influenza pandemic. By performing these projects a relevant disease model will be developed to test various influenza strains of varying potency (including various pandemic strains). This model will also allow for a working collaboration for testing pregnant animals for other respiratory pathogens of high bio-security importance (such as anthrax, smallpox, plague, etc.). This is to our knowledge the only investigations into the pregnancy-specific characteristics of these threatening diseases, and having a relevant animal model will allow us to form a basis for future funded research studies potentially using non-human primates.

Eventually, components of what we learn and test will have human relevance in terms of pregnant women's response to such infections. It may also lead to potential ways to prevent disease through vaccination and to treat such infections in pregnant women. It is important to note that pregnant women are an often forgotten population in terms of research in this area yet are a crucially important sector of the population for many reasons. This research has potentially far reaching implications for societal benefit and protection, as this project represents concrete steps in strengthening this important collaboration between investigators and in developing this animal model on which to build.

Summary of Research Completed

1. Experiment 1: Determination of 2009 H1N1 virulence in pregnant ferret model:

Methods:

For experiment 1, we used a total of 14 ferrets (1/2 pregnant and timed in pregnancy) that were obtained from the vendor at approximately 28 days gestation. They were acclimated for 5 days and then were implanted with temperature and ID microchips. They were then split into 4 groups of 3 ferrets each that were exposed to 2 different doses of 2009 H1N1 by aerosol challenge on day 32 of gestation. In addition, we used a control group of 2 same gestational age pregnant sham-exposed ferrets to assist in comparing pregnancy outcomes.

2009 H1N1 influenza was grown in MDCK cells. Titration of influenza was performed in a $TCID_{50}$ assay using MDCK cells. The actual doses used for the aerosol challenges with 2009 H1N1 were: *Low Dose* 150 (+/- 107) or *High Dose* 1504 (+/- 339) $TCID_{50}$. Exposures were performed inside a class III biological safety cabinet using the AeroMP aerosol control platform (Biaera Technologies) and Collison nebulizers (BGI). All ferrets were then followed for 10 days to document disease course. Ferrets that became moribund were euthanized and the tissues were collected and frozen for subsequent virologic and pathologic evaluation with future funding.

Results:

The first measured endpoint was % weight change from baseline pre-challenge as a measure of overall health after challenge. This is an accepted endpoint for such aerosol challenges.

Figure 1 represents the pregnant ferrets % weight change after challenge and graphically displayed up until delivery. It is important to remember that pregnant ferrets are supposed to gain weight due to the gestation. Unfortunately, the 2 sham exposed ferrets required euthanasia due to non-influenza related illness and therefore can't be used for comparison. This was likely due to travel and acclimatization issues.

Overall, it is clear from this small experiment that the exposed pregnant ferrets lost weight. The data is not shown but these ferrets also demonstrated a febrile response and had clear influenza clinical illness that manifested as profuse nasal congestion/copious mucus production. In comparison, the non-pregnant ferrets did have a mild febrile response, but did not demonstrate other clear signs of influenza illness such as nasal congestion or respiratory illness. In addition,

one high-dose pregnant ferret required early euthanasia due to severe respiratory distress and lethargy.

Below in Figure 2 are the % weight gain/loss data for the non-pregnant ferrets. These data demonstrate clearly that the non-pregnant ferrets did not lose weight, and in fact gained weight. In addition, the overall lack of clinical disease among non-pregnant ferrets compared to pregnant ferrets was striking.

In terms of births, the average number of kits per mother ferret (N=7 for both groups) was not different between the low and high dose ferrets. In addition, the average weight of the litters and the survival of kits also were not different between the 2 dose groups. Due to the lack of sham infected mothers surviving beyond 2 days, it is difficult to draw any meaningful conclusions about kit size, weight or survival.

Summary of Experiment #1:

These data, while limited by the lack of pregnant control (sham exposed) data, strongly suggest that the pregnant ferrets contracted influenza at less of a challenge dose and manifested clearly worse signs of disease compared to the non-pregnant ferrets. This is an excellent foundation in which to expand our investigations because this is a model that appears to mimic what is seen in human pregnancy.

2. Experiment 2: Pathogenesis of 2009 H1N1 in a pregnant ferret model:

We proposed the performance of the following project:
28 ferrets (1/2 pregnant and timed in pregnancy), certified influenza seronegative will be gotten at approximately 28 days gestation. They will be acclimated for 5 days and they will be implanted with temperature and ID microchips. Ferrets will then be exposed to a dose 100X the EC_{50} (determined from experiment #1). On days 0,2,4,7 animals will be serially euthanized and necropsied to take samples for virologic and pathologic evaluation (2 on day 0, then 4 each on days 2, 4 and 7).

We proceeded with ordering the timed pregnant ferrets (as well as non-pregnant ferrets) from the vendor in November, 2010, after the first experiment was completed to perform this planned experiment. Unfortunately, however, we learned from other investigators within our institution that many of the ferrets obtained from the same vendors were seropositive for 2009 H1N1 (previously infected, and thus not usable for challenge pathogenesis studies).

In light of these findings, we queried the vendor about the ferrets (both pregnant and non-pregnant) that we had already ordered for the 2nd experiment (and paid for) and learned after testing that our ferrets were also seropositive for 2009 H1N1. Thus, we canceled the order given the lack of suitability for the pathological challenge studies. We have since received a refund on that order and have obtained a contract with an alternative vendor using these funds. Currently, we are in the process of working collaboratively with the new vendor to test the new ferrets for seropositivity to 2009 H1N1. Once we confirm seronegativity to 2009 H1N1, we will receive the

shipment and perform the proposed challenges and pathological investigations. This is projected to take place in the spring of 2011.

Figure 1, % Weight Change (Pregnant)

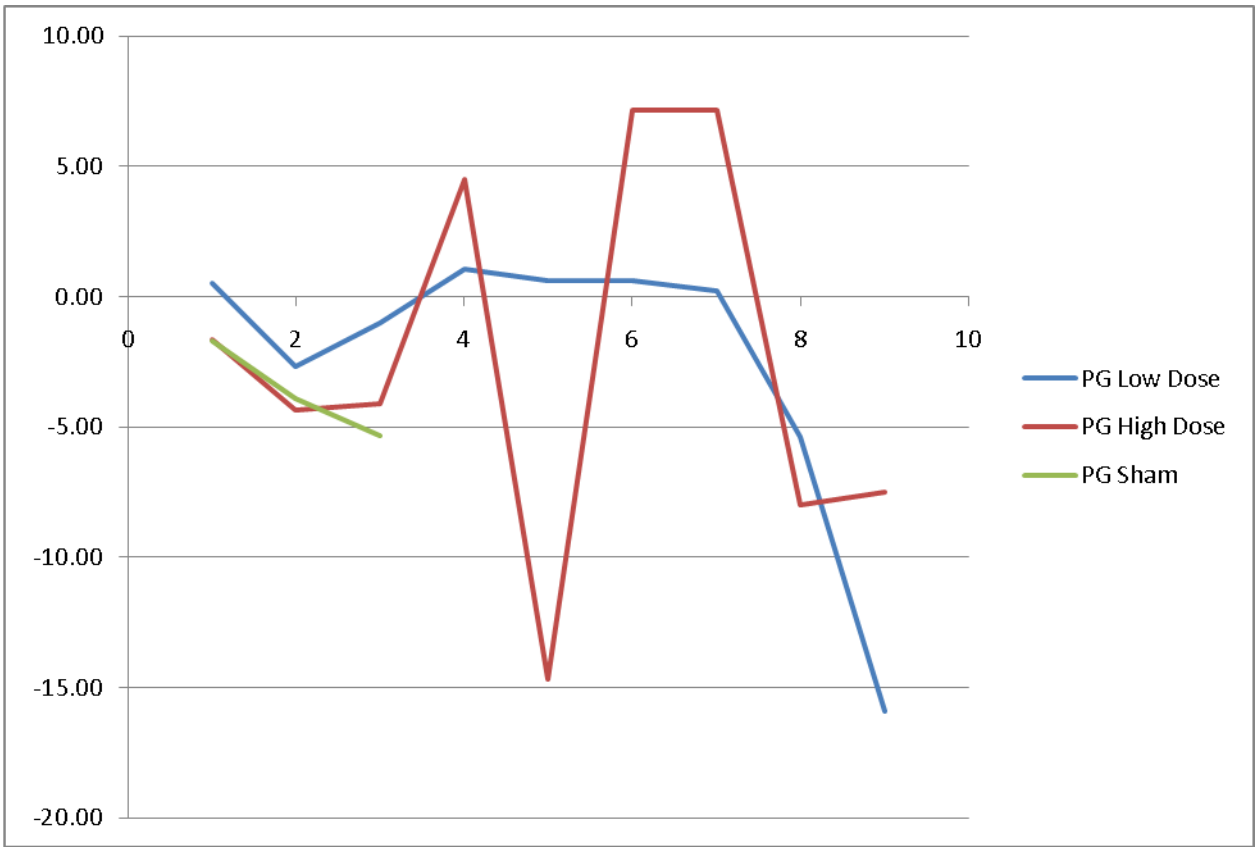

Figure 2, % Weight Change (Non-pregnant)

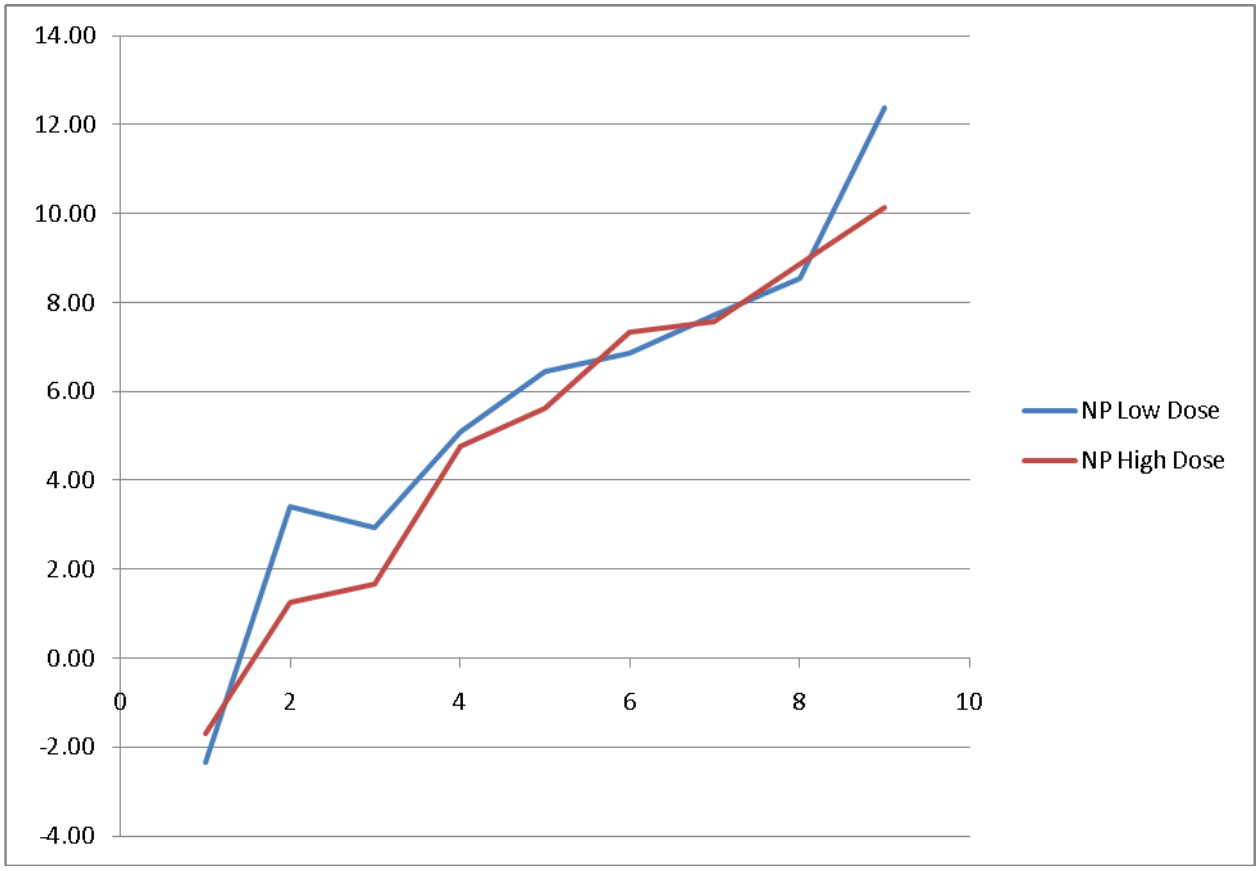

Research Project 2: Project Title and Purpose

Relationships among PPAR gamma Activity, Hypoxia, and Differentiation in Human Placenta - The main purpose of this study is to understand the relations among four important biological processes occurring in human placenta: placental hypoxia, normal trophoblast differentiation, peroxisome proliferator-activated receptors (PPAR) gamma activity, and fetal growth restriction. By applying various statistical procedures to both historic and recently generated data sets, the results of this study could deepen our understanding of these placental processes from the genomic point of view, shed light on the mechanism behind the fetal growth restriction caused by hypoxic injury, and eventually facilitate the development of prevention and treatment methods for fetal growth restriction.

Duration of Project

1/1/2010 - 12/31/2010

Project Overview

Fetal growth restriction (FGR) has been shown to result in fetal morbidity and mortality, as well

as later health complications for adult survivors. One of the main risk factors of FGR is believed to be hypoxia, which may prevent trophoblast differentiation, enhance trophoblast apoptosis, and hence contribute to fetal growth restriction.

Peroxisome proliferator-activated receptors (PPAR) gamma is a transcription factor playing an important role in placental development and function. On one hand, a mouse model study shows that a PPAR gamma null murine placenta fails to terminally differentiate and is not permeated with fetal vessels; yet on the other hand, an in vitro study shows that PPAR gamma ligand troglitazone modulates trophoblast differentiation and attenuates trophoblast apoptosis under hypoxia condition.

Given the close relations among hypoxia, fetal growth restriction, trophoblast differentiation, and PPAR gamma activity, it is natural to ask if there are sets of genes whose expression patterns could explain both the close relationships and the dissimilarities among these processes. Moreover, assuming the pivotal role of hypoxia in FGR, it would also be interesting to know if there is a specific course of hypoxia during later stages of gestation that is responsible for most of the observed fetal growth restriction.

To answer these questions, in this project, I will conduct an exploratory study of the relationships among the transcriptomes of undifferentiated trophoblast, differentiated trophoblast (under normal condition), trophoblast under hypoxia, and trophoblast treated with PPAR ligands, as well as placentas from normal and FGR pregnancies. Both supervised and unsupervised statistical learning procedures will be employed. The data of this study include historical microarray gene expression data for primary trophoblast cell samples that are allowed to differentiation under normal condition, or treated with hypoxia, or treated with PPAR gamma ligands, as well as microarray data for both normal and FGR placenta. The microarray data are supplemented by recently generated qPCR data of 24 selected genes for normal and FGR placentas, and trophoblast cells treated under various hypoxia schemes.

Principal Investigator

Tianjiao Chu, PhD
Assistant Professor
University of Pittsburgh
204 Craft Ave., B409
Pittsburgh, PA 15213

Other Participating Researchers

Yoel Sadovsky, MD - employed by University of Pittsburgh

Expected Research Outcomes and Benefits

Through the exploratory study of the relationships among trophoblast differentiation, hypoxia, PPAR activity, and fetal growth restriction, this study should be able to identify both the sets of genes whose expression patterns may reveal both the connection and dissimilarity among

hypoxia, trophoblast differentiation, PPAR gamma activity, and fetal growth restriction, and the genomic functional groups overrepresented in each set of these genes.

Moreover, by analyzing the qPCR data of the expression levels of a selected set of 24 genes in both in vivo conditions and in vitro conditions, this study could enable us to identify a specific course of hypoxia that is most likely responsible for the fetal growth restriction.

Ultimately, the results of this study will improve our understanding of the mechanism of hypoxic injury to placenta and the role PPAR gamma activity in regulating placental development and provide insight on the connection between hypoxia and fetal growth restriction, therefore aiding in the prevention and treatment of fetal growth restriction.

Summary of Research Completed

In the second stage of this project, following the study plan, I analyzed the gene expression profiles of primary human trophoblast (PHT) cells during differentiation, under hypoxia, treated with PPAR gamma ligands, as well as the gene expression of placentas from pregnancies with fetal growth restriction (FGR), and performed gene ontology analysis to identify the main functions for the genes differentially expressed under various treatment conditions.

A. Differential expression analysis and gene ontology analysis

A1. Identify genes differentially expressed in PHT cells treated with PPAR gamma agonists

In the first microarray whole genome transcription data set M1, two samples of PHT cells were treated respectively with PPAR gamma agonists GW 7845, or PPAR gamma agonist troglitazone, while another PHT sample was untreated. Five technical replicates from each sample were hybridized to Affymetrix Human U95 A-E chip sets. We used Robust Multi-array Analysis (RMA) algorithm to normalize and summarize the probe set intensity values. Then empirical Bayesian algorithm, implement in the R package “limma”, was applied to test, for each gene, if it was differentially expressed between untreated trophoblast cells and trophoblast cells treated by GW 7845 or troglitazone. The limma algorithm assumes an inverse Chi-square prior distribution for the within group variances of the genes, estimates the hyper parameters of the prior using the empirical Bayesian method, then performs a moderated student’s t test using the posterior mean of the within group variance and moderated degrees of freedom. The Storey’s qvalue method was used to calculate the adjusted p values to control the false discovery rate.

With false discovery rate controlled at 5%, we found 26 genes that are down regulated both when the PHT cells were treated with GW 7845, and when treated with troglitazone, while 17 genes were up regulated. We used one-tail Fisher’s exact tests to identify the gene ontology terms in the biological processes (BP), molecular functions (MF), and cellular components (CC) categories, and set the cutoff p value at 0.0001. Table 1 gives the BP terms overrepresented in genes up/down-regulated by the two PPAR gamma agonists.

A2. Identify genes differentially expressed in PHT cells after 48 hours differentiation

In the second experiment, we studied the dynamics of the gene expression profile of PHT cells during differentiation. PHT cell samples were collected at 0, 24, 48, and 72 hours during differentiation. One sample from each time point was hybridized to the Affymetrix Human U95 A-E chip set. The main goal of the analysis of this data set is to find the relation in gene expression between differentiation and hypoxia. Because our hypoxia data were generated from samples treated under hypoxic condition for 48 hours (see next section), here we focused on the identification of the genes differentially expressed between 0hr and 48hr after differentiation.

Upon review, we noticed that there was only a single sample of the PHT cells from the control group and a single sample from the treatment group, and there was no technical replicate; we therefore could not estimate the within group variance of each gene, and hence were unable to test directly if any gene was differentially expressed at 48h of differentiation. However, in the previous PPAR gamma agonists experiment, there were 5 replicates of the trophoblast sample in the control group. Given that the samples in the previous experiment are very similar to the samples in this differentiation experiment, we decided to include the 5 technical replicates of the control group from the PPAR gamma agonists experiment in the analysis of this differentiation experiment. We used RMA algorithm to normalize and summarize the probe set intensity values, then applied the limma algorithm to test, for each gene, if it was differentially expressed between 0 hour and 48 hours. The within group variances needed for the moderated t test were estimated from the 5 technical replicates borrowed from the PPAR gamma agnoists experiment. The p values of the tests were adjusted using the qvalue method.

With false discovery rate controlled at 5%, we found 1651 genes that are up regulated at 48 hours of differentiation, and their observed signals at 24 hours and 72 hours were higher than at 0 hour. We also found 1373 genes down regulated after 48 hours of differentiation, and their observed signals at 24 hours and 72 hours were lower than at 0 hour. We used one-tail Fisher's exact tests to identify the BP, MF, and CC terms. Table 2 gives the BP terms overrepresented in genes up/down-regulated at 48 hours of differentiation, with p values less than or equal to 0.0001.

A3. Identify genes differentially expressed in PHT cells after 48 hours exposure to hypoxia

In the third experiment, which will be called the hypoxia experiment, we studied the gene expression profile of PHT cells under hypoxia. Three PHT cell samples were collected, each sample was divided into two parts, and subjected to 0% oxygen and 20% oxygen respectively for 48 hours. All samples were hybridized to the Affymetrix Human U95AV2 chip.

We used RMA algorithm to normalize and summarize the probe set intensity values, obtained the pair-wise difference in the log expression level of each gene between the normal and hypoxic treatment of each sample. Then we applied the limma algorithm to determine whether it was differentially expressed between normal and hypoxic conditions by testing if the pair-wise difference obtained previously for each gene was not equal to 0. The p values of the tests were adjusted using the qvalue method.

With false discovery rate controlled at 5%, we found 40 genes up regulated under hypoxic condition, and 110 genes down regulated under hypoxic condition. We used one-tail Fisher's exact tests to identify the BP, MF, and CC terms. Table 3 gives the BP terms overrepresented in genes up/down-regulated under hypoxic condition, with p values less than or equal to 0.0001.

A4. Identify genes differentially expressed in placentas from normal and FGR pregnancies

In the last experiment, which will be called the FGR experiment, 3 normal and 3 FGR placenta were collected. All samples were hybridized to an Affymetrix Human U95AV2 chip. RMA algorithm was used to normalize and summarize the probe set intensity values. We used limma algorithm to test, for each gene, if it was differentially expressed between normal and FGR placenta. The p values of the tests were adjusted using the qvalue method. With false discovery rate controlled at 5%, we found no genes significantly differentially expressed. We then used one-tail Fisher's exact tests to identify the BP, MF, and CC terms for those genes with p value less than or equal to 0.01. No significantly overrepresented BP terms were found with p values less than or equal to 0.0001.

B. Relations among PPAR gamma agonists, differentiation, hypoxia, and FGR

B1. Pair wise dependency in differentially expressed genes among PPAR gamma agonists, differentiation, hypoxia, and FGR

The main goal of this project was to study the relations among PPAR gamma, differentiation, hypoxia, and FGR. For this purpose, for each pair of experiments, we identified the genes differentially expressed in both experiments (for the FGR experiment, we used the genes with p values <= 0.01), then created a 2 by 2 contingency table for these genes with two factors: The first factor is whether a gene is up or down regulated in the first of the two experiments, the second factor is whether a gene is up or down regulated in the second of the two experiments. We then used two-tail Fisher's exact test to determine if the probability that a gene is up regulated in one experiment is dependent on whether it is up regulated in the other experiment.

From the 4 experiments, we made 6 pairs, and created 6 contingency tables. Only in the contingency table for the differentiation and hypoxia experiments (Table 4) did we obtain a significant p value (<= 2.2E-16). Table 4 shows that among genes differentially expressed in both experiments, genes up-regulated at 48h differentiation are very likely to be down regulated under hypoxia, and genes down-regulated at 48h differentiation are very likely to be up-regulated under hypoxia. This suggests an extremely strong negative relation in gene expression dynamics in PHT cells between the differentiation and hypoxia.

B2. Pair wise dependency in BP terms overrepresented in differentially expressed genes among PPAR gamma agonists, differentiation, hypoxia, and FGR

Using a similar approach as used in the previous section, we studied the pair wise dependency in BP terms overrepresented in differentially expressed genes among PPAR gamma agonists, differentiation, hypoxia, and FGR. For each pair of experiments, we first identified the BP terms over-represented in genes differentially expressed in both experiments, using one tail Fisher's

exact test. For the FGR experiment, we selected the BP terms with p values <= 0.01, for other experiments, we selected the BP terms with p values <= 0.001. We then created a 2 by 2 contingency table for these BP terms with two factors: The first factor is whether a BP term is overrepresented in genes up or down regulated in the first of the two experiments; the second factor is whether a BP term is overrepresented in genes up or down regulated in the second of the two experiments. We then used two-tail Fisher's exact test to determine if the probability that a BP term is overrepresented in genes up regulated in one experiment is dependent on whether it is overrepresented in genes up regulated in the other experiment.

Out of the 4 experiments, we made 6 pair-wise comparisons, and created 6 contingency tables. None of them show significant dependency. Moreover, we found none of the BP terms overrepresented in genes differentially expressed between normal and FGR placentas are overrepresented in genes differentially expressed in any of the other three experiments. This further confirms our finding in aim 2 of this project that the expression profile of PHT cell in vitro is very different than the expression profiles of either normal or FGR placenta in vivo.

Table 1: BP terms overrepresented in genes regulated by PPAR gamma agonists

Up Regulated Genes	Down Regulated Genes
parturition	regulation of epithelial cell differentiation
	monocyte chemotaxis
	negative regulation of programmed cell death
	anti-apoptosis

Table 2. BP terms overrepresented in genes differentially expressed at 48h differentiation

Up-regulated @ 48h	Down-regulate @48h
vesicle-mediated transport	translational elongation
ER to Golgi vesicle-mediated transport	regulation of programmed cell death
female pregnancy	death
macromolecule catabolic process	negative regulation of cell death
modification-dependent protein catabolic process	negative regulation of biological process
	mitosis
	cell division
	positive regulation of cell death
	organelle fission
	anti-apoptosis
	cell junction assembly
	positive regulation of protein metabolic process
	macromolecular complex subunit organization
	regulation of cellular component movement
	DNA replication
	positive regulation of signal transduction
	actin cytoskeleton organization
	cell motility
	positive regulation of cellular metabolic process
	mitotic cell cycle
	blood vessel development
	cell cycle process
	induction of apoptosis
	regulation of cellular protein metabolic process
	regulation of cellular component organization
	ruffle organization
	organ development
	protein complex assembly
	M phase
	response to wounding
	hemidesmosome assembly
	negative regulation of transcription factor activity
	regulation of protein kinase cascade
	response to DNA damage stimulus
	negative regulation of cell proliferation
	microtubule-based process
	cell-substrate adhesion
	DNA replication initiation

Table 3. BP terms overrepresented in genes diffierentially expressed under hypoxia

Up regulated under hypoxia	Down regulated under hypoxia
taxis	female pregnancy

Table 4. Genes differentially expressed in both differentiation and hypoxia experiments

Number of Genes	Up regulated under hypoxia	Down regulated under hypoxia
Up regulated at 48h Differentiation	0	96
Down regulated at 48h Differentiation	27	1

Research Project 3: Project Title and Purpose

Hypoxia Inducible miR-210 as a Potential Therapeutic Target in Renal Cell Carcinoma - We plan to illustrate the mechanism of apoptosis in clear cell renal cell carcinoma cells (ccRCC) harboring *VHL* mutation caused by inhibition of a hypoxia inducible microRNA (miRNA), miR-210. By identifying the genes responsible for this phenotype, we will discover potential novel therapeutic targets for ccRCC, which is refractory to current chemo- and radiation- therapies.

Duration of Project

1/1/2010 – 12/31/2010

Project Overview

The main objective of this project is to systematically investigate the mechanism of a hypoxia inducible miRNA, miR-210, on ccRCC tumor survival and to examine miR-210 or its target genes as novel therapeutic targets for ccRCC. We have planned a series of mechanistic studies using paired ccRCC cell lines, ccRCC cells with *VHL* mutation ($VHL^{-/-}$, with highly elevated miR-210 expression) and same ccRCC cells expressing reconstituted wild type *VHL* ($VHL^{+/+}$, with basal low level miR-210 expression). Specifically, we will examine cell survival, proliferation, apoptosis, and metabolism after inhibiting miR-210 expression in $VHL^{-/-}$ cells. In addition, we will identify miR-210 targets in these cells by Argonaute 2 immunoprecipitation followed by microarray experiments and will manipulate these identified genes by either shRNA knock-down or ectopic expression to recapitulate the phenotype of miR-210 knock-down, increased apoptosis. Finally, we will investigate the effect of inhibition of miR-210 expression on the sensitivity of ccRCC cells to chemotherapeutic agents. In summary, this project is intended to provide mechanistic insights on miR-210's function in ccRCC survival and to identify novel therapeutic targets for ccRCC.

Principal Investigator

Xin Huang, PhD
Research Assistant Professor
Magee-Womens Research Institute and Foundation
204 Craft Ave., B407
Pittsburgh, PA 15213

Other Participating Researchers

None

Expected Research Outcomes and Benefits

ccRCC is among the tumors most resistant to radiation- and chemo-therapies. Currently, there is no effective treatment for this devastating disease. Our project will address the function of miR-210 in ccRCC apoptosis and survival and illustrate the mechanism of cell death caused by miR-210 inhibition. We expect to identify a list of miR-210 target genes, of which ccRCC cells must repress when the tumor suppressor gene, *VHL* is mutated. These miR-210 target genes or miR-210 *per se* will be attractive targets for developing novel therapy against ccRCC and eventually leading to a better overall survival of ccRCC patients.

Summary of Research Completed

<u>Down-regulating miR-210 expression induces phospho-p53 (S15) and p27 expression</u>

The *TP53* gene is a major tumor suppressor gene in human genome. The protein product of *TP53*, p53, is a master regulator of cell cycle progression and apoptosis. Because of the significantly slower cell proliferation after miR-210 knockdown, we reasoned that p53 may be responsible for it. Since ATM and ATR kinases can phosphorylate p53 at serine 15 (S15), which stabilize p53 and leads to cell cycle arrest, we examined the status of phospho-p53 (S15). As expected, phospho-p53 (S15) is highly upregulated after miR-210 knockdown in RCC4 cells (Figure 1). We also examined two major downstream targets of p53 involved in cell cycle regulation, p21 and p27. There was no change on p21 expression detected. However, a significant increase of p27 was detected by Western blotting. Currently, we are performing cell cycle and microarray experiments after miR-210 knockdown to further elucidate the mechanism of miR-210 function in RCC4 cells.

<u>Identifying miR-210 target genes</u>

The experimental strategy to identify miR-210 targets in RCC4 cells is illustrated in Figure 2. Immunoprecipitated mRNA samples have been sequenced at the University of Pittsburgh Genomics and Proteomics Core Facility (GPCL). More than 60 million reads have been collected for each IPed sample. But due to the extremely large volume of data acquired by SOLiD sequencing, the data analysis is still ongoing at the Bioinformatics Core at GPCL.

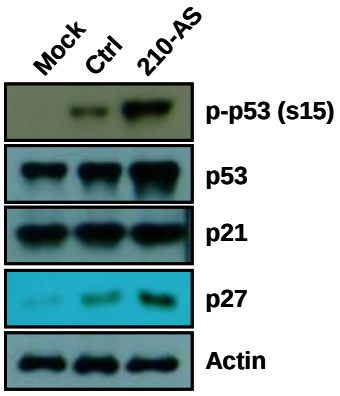

Figure 1. *Inhibition of miR-210 in RCC4 cells results in increased phosphor-p53(S15) and p27.*

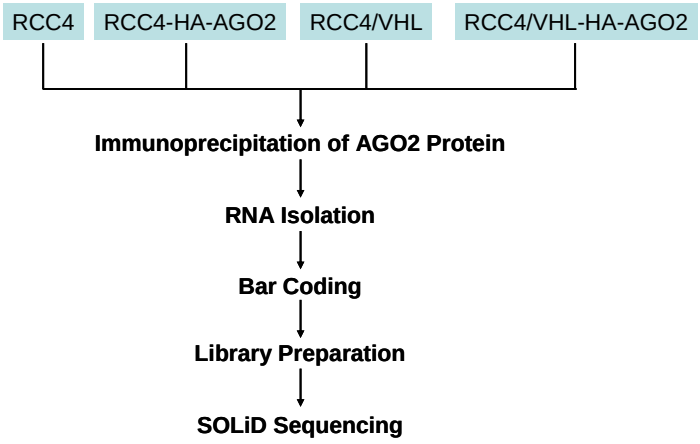

Figure 2. Strategy for identifying miR-210 target genes in RCC4 using AGO2 immunoprecipitation and next generation sequencing. Schematic illustration of the strategy to identify miR-210 targets in RCC4 cells.

Research Project 4: Project Title and Purpose

Role of miR-424 in the Differentiation and Function of Placental Trophoblasts - Our ultimate goal is to understand how hypoxic stress impacts placental function. Feto-placental hypoxia is associated with pregnancy complications but the molecular mechanisms remain poorly understood. We recently found that hypoxia induces major changes in the expression levels of several microRNAs (miRNAs), a family of small regulatory RNAs that are increasingly found linked to disease. One of them, mir-424, is normally abundant in placental trophoblasts but is significantly decreased when cells are exposed to hypoxia. The downregulation of miR-424 could lead to the de-repression of a number of target genes and have profound consequences on the trophoblast biology. This research will focus on the expression and the role of miR-424 in the differentiation of placental trophoblasts.

Duration of Project

1/1/2010 - 12/31/2010

Project Overview

Placental insufficiency is one of the main complications of pregnancy and is associated with compromised fetal development and poor outcome. Failure of the placenta to fulfill its function is often associated with feto-maternal hypoxia. Whereas incompletely understood, recent studies have shown that hypoxic stress significantly alters gene expression in placental trophoblasts and impairs their differentiation. In order to interrogate the molecular changes brought about by hypoxic stress, we recently performed several miRNA profiling experiments in human primary trophoblasts that were cultured in either standard oxygen conditions (FiO_2=20%) or in hypoxic conditions (FiO_2=1%). Among a set of differentially regulated miRNAs we found that miR-424, a normally abundant miRNA, is significantly reduced in hypoxic trophoblasts. As miRNAs have the potential to regulate many target genes, this could affect differentiation pathways of trophoblasts. Consistent with this hypothesis, we identified two targets of miR-424 that were downregulated in placental trophoblasts exposed to hypoxia. In the genome, miR-424 is found in an intergenic region located on the chromosome X and in a cluster with five other miRNA genes that may be co-regulated. This feature may even further expand the regulatory potential of the miRNAs from this genomic region. Interestingly, this cluster is conserved across mammals including the mouse and we detected several miRNAs from this region in mouse placentas. It is our hypothesis that hypoxia affects the expression of several members of this miRNA cluster leading to the de-repression of several genes involved in the control of trophoblast differentiation. To test this hypothesis we will first analyze the impact of miR-424 on the cellular functions of primary trophoblasts. To this end we will inhibit the function of miR-424 and some of its targets in trophoblasts and analyze the cellular consequences. Finally, we will further characterize the expression profile of this cluster in the human placenta as well as the mouse placenta.

Principal Investigator

Jean-Francois Mouillet, PhD
Research Instructor
University of Pittsburgh
Department of OBGYN and Reproductive Sciences
Magee-Womens Research Institute
204 Craft Avenue, Room A634
Pittsburgh, PA 15213

Other Participating Researchers

Yoel Sadovsky, MD, Magdalena Jennings - employed by University of Pittsburgh

Expected Research Outcomes and Benefits

Our long-term goal is to understand the response of the human placenta to injury, and in particular to low oxygen (hypoxic) stress. This knowledge will pave the way for the design of new preventive measures to decrease the impact of placental injury on the developing fetus. Low placental oxygenation is one of the main stress conditions in the human placenta and is believed to play a role in the development of pathologies such as intrauterine growth restriction (IUGR) and hypertension of pregnancy. These conditions are associated with increased perinatal illnesses and mortality. Newborns surviving these insults are at risk for lifelong complications, including developmental diseases and a greater incidence of the adult metabolic syndrome (type-2 diabetes, high lipids, hypertension, obesity and related illnesses). Despite the well-documented association between hypoxia and these conditions, little is known about the mechanisms involved in the development of these defects.

Oxygen plays a major role in the differentiation of placental cells that occurs during pregnancy. We recently performed several experiments of placental cells cultured in low oxygen conditions to mimic placental hypoxia and examined changes in gene expression. This screen led to the identification of several genes including small RNA molecules (called microRNAs) whose expression is altered in hypoxia. In this project we focus on a novel pathway of gene regulation in the human placenta centering on regulation in the context of hypoxia. Results from our experiments on miR-424 are likely to advance our knowledge on previously unknown pathways that are activated during hypoxia and their role in placental response to injury.

Summary of Research Completed

The goal of this project was to investigate the function of microRNA-424 (miR-424) in placental trophoblasts. Mir-424 is a mammalian-specific miRNA particularly abundant in placental cells but with an unknown function. We recently identified miR-424 in a microarray-based screen for miRNAs that are differentially regulated in hypoxic human trophoblasts. In this assay, miR-424 was among the few species that were consistently downregulated in hypoxia. We therefore hypothesized that reduced levels of miR-424 could lead to the derepression of its targets and impact the biology of trophoblasts.

In the last six months of funding for this project, we have made the following progress on the specific aims described in the original research plan:

<u>Aim 1</u>: Analyze the impact of miR-424 on the cellular functions of primary trophoblasts.

During the first phase of the project we identified and confirmed FGFR1 as one of the targets for miR-424. We also identified the sequence within the 3'UTR of FGFR1 that mediates the silencing by this miRNA. In the second phase we pursued our experiments aiming at further characterizing the functional interaction between the two entities.

As a preparation for the functional characterization of miR-424 in primary trophoblasts we measured FGFR1 levels in cells exposed to hypoxia. Primary trophoblasts were isolated from different placentas and cultured in 20% O_2 and 1% O_2 for 48 h before harvest. In one series of

experiments, total RNA was isolated and a real-time qPCR was performed to determine FGFR1 mRNA levels in standard conditions and hypoxia. In a second series we measured FGFR1 at the protein level by western blot. At the transcript level we observed a sharp increase of FGFR1 in primary trophoblasts cultured in hypoxia (Fig. 1A). Similarly, we detected a consistent two-fold increase of FGFR1 in western blot (Fig.1B).

In order to further validate the role of miR-424 in the silencing of FGFR1 we conducted a series of experiments in which we sought to inhibit the function of miR-424. We first used a technique based on the transfection of a modified antisense oligonucleotide (ASO) acting as an antagonist to miR-424. The trophoblast-derived HTR8/SV cell line was transfected with a miR-424 sensor construct based on the psiCHECK2 vector (Promega) containing three artificial miR-424 target sites. In addition to the reporter construct we also co-transfected a miR-424 antisense oligonucleotide obtained from Dharmacon/Thermo. Cells were transfected using DharmaFECT Duo reagent (Dharmacon/Thermo) that was optimized for the cotransfection of plasmids and oligonucleotides. After 48 h of incubation cells were harvested and assayed for luciferase activity using the Dual Luciferase Assay (Promega). Despite previous successes using this approach on different miRNAs, our attempt to knockdown miR-424 was rather disappointing and only a modest effect was detected. Curiously, a slightly more important relief of luciferase activity was observed when cells were transfected with a vector expressing miR-424. This could be the consequence of the accumulation of high levels of the luciferase reporter in transiently transfected cells where endogenous levels of miR-424 are not high enough to significantly impact luciferase expression. In this case only overexpression of miR-424 would permit detection of a silencing effect on the reporter. Because of this potential saturating effect it was difficult to assess the inhibitory potential of this antisense oligonucleotide in this experimental setup. Although these preliminary knockdown experiments were not conclusive we tried to transfect primary human trophoblasts (PHTs) with the miR-424 inhibitor and analyzed biological consequences. In this system we do not rely on the expression of a transfected reporter gene but rather monitor the effect of miR-424 inhibition of trophoblast differentiation. PHTs cells were seeded in 6-well plates and transfected with a miR-424 inhibitor or a scrambled oligonucleotide as a control using DharmaFECT 1 reagent. Cells were further incubated for 48 h after transfection, and 1 ml of culture medium was collected for human chorionic gonadotropin (hCG) level measurements. As PHT cells differentiate into syncytium *in vitro* they release increasing amounts of hCG. We routinely monitor hCG production by EIA to assess the differentiation status of our cells. No change in hCG release was observed after transfection of a miR-424 inhibitor or a control oligonucleotide. We also harvested the cells and performed qRT-PCR, which showed no change in miR-424 levels after transfection, indicating that the ASO failed to significantly reduce miR-424 levels. We also tested a new type of LNA-based ASO recently marketed by Exiqon and referred to as miRCURY LNA™ microRNA Power Inhibitors. Although this new product led to potent inhibition of several miRNA species in our system, it failed to produce significant inhibition of miR-424 in primary trophoblasts.

In the absence of significant miR-424 suppression using an ASO, we decided to take a different approach and use the technique of miRNA sponge. The technique is based on overexpressing a transcript whose sequence contains multiple copies of a specific miRNA binding site. Each sponge transcript is able to bind and sequester several miRNA copies therefore acting as competitive inhibitors of miRNAs. To assemble the sponge we sequentially cloned 4 copies of

an oligonucleotide containing two miR-424 binding sites into the pIS0 vector. The final sponge cassette containing 8 copies of miR-424 target sequences was PCR amplified and cloned into the pCMV-d2eGFP vector to be expressed under the control of a CMV promoter. We first placed the sponge into a regular plasmid in order to test its efficacy in the HTR8 cell line. The miRNA sponge was tested on both the miR-424 sensor and the FGFR1-3'UTR reporter. In both cases we observed an increase of the reporter luciferase activity when the cells were transfected with increasing amounts of the sponge. However, although consistent, the silencing relief brought about by the sponge was relatively weak and never exceeded an increase of more than 30% with respect to the basal luciferase activity detected in absence of the sponge (Fig.3). This level of miRNA suppression is considerably lower than those reported in the literature and did not bode well for the inhibition of miR-424 in primary cells.

Aim 2: Examine the expression of miR-424 and associated species in the human and mouse placenta.

During the second phase of this project we investigated the miR-424 cluster expression in the human and mouse placenta. We first asked whether the miRNAs in the close proximity of miR-424 were co-regulated. Primers specific to each member of this cluster were designed and used to compare their individual expression in human primary trophoblasts cultured in normoxia and hypoxia. Although several species were barely detectable, they all showed the same trend where each was reduced in hypoxic trophoblasts (Fig.4). This similar pattern of variation in their expression suggests that this family of miRNAs belongs to a cluster of co-regulated genes.

As in humans, miR-322 (the mouse miR-424 ortholog) is primarily expressed in placental tissue. We also detected the expression of other miRNAs (miR-351, and miR-450) that are part of the cluster in the mouse placenta (Fig. 5). These observations support the idea that these miRNAs are important for the placental function and also designate the mouse as a promising model for the study of the role of this cluster in the biology of the placenta.

Previous experiments showed that miR-424 expression is altered in human trophoblasts that are exposed to hypoxia. We next tested the effect of hypoxic stress on the expression of placental miR-424/322 in mice. For this experiment, pregnant mice at gestational age 11.5 were placed into a hypoxia chamber containing 12% oxygen for four days (until gestational age 17.5). This treatment has been used in our laboratory to study the effect of hypoxia on fetal development. Although mice are exposed to low oxygen concentration for only four days it is sufficient to impact the development of fetuses that typically show lower body weight when compared to fetuses from mice housed in normal oxygen conditions. Surprisingly, we did not see a decrease of miR-424/322 expression but rather an increase in the placentas from mice housed in hypoxic conditions (Fig. 6). Since the whole placenta contains many cell types in addition to trophoblasts it will be important to determine whether this increase of miR-424/322 levels originates in trophoblasts or other cell types.

To further analyze miR-424 expression in the mouse placenta we performed *in situ* hybridization (ISH) on frozen sections using a DIG-labeled LNA probe. Dissected mouse placentas were pre-fixed in 4% paraformaldehyde (PFA) in phosphate buffered serum (PBS) overnight, then successively in 10% sucrose in PBS for 30 min, 20% sucrose in PBS and finally mounted in

Tissue-Tek OCT (Sakura Finetek). Frozen sections (10 μm) were treated with 20 mg/ml proteinase K (Roche), then fixed in 4% PFA and acetylated for 10 min with a mixture of 0.25% acetic anhydride and 0.1 M triethanolamine. The postfixed tissues were subsequently incubated overnight with DIG-labeled LNA probes from Exiqon (Exiqon) according to the manufacturer's instructions. After stringent washes, the slides were incubated with alkaline phosphatase conjugated with an anti-DIG antibody (Roche) and detected using BM Purple Substrate (Roche). Finally the slides were mounted in DPX (Fluka). In addition to miR-322/424, we also probed our slides for miR-205 and miR-335, two miRNAs that are abundant in the placenta and can serve as positive controls. We detected a strong signal throughout the placenta with probes complementary to miR-205 and miR-335 (Fig. 7). However, miR-322/424 generated only a weak signal in some localized areas of the placenta, mainly in the labyrinth layer. Despite varying the hybridization conditions we could not obtain a strong and clear signal with miR-322. This result was unexpected in light of the high expression of this miRNA species usually detected in the placenta. In contrast, we obtained strong staining with probes directed against similarly highly expressed miRNAs in the mouse placenta, including miR-205 and miR-335. The reason of this weak signal is currently unknown.

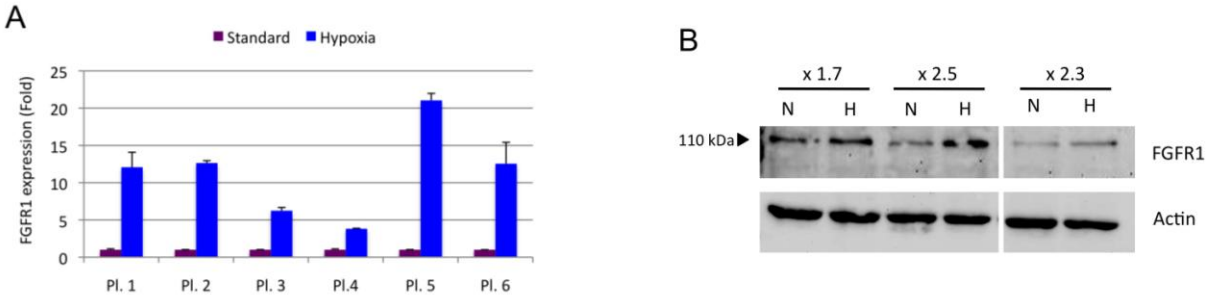

Fig. 1: Expression of FGFR1 in hypoxic trophoblasts. A) Real-time qPCR analysis of FGFR1 mRNA levels in primary trophoblasts from 6 different placentas (Pl.1 to Pl.6). B) Western blot analysis of FGFR1 (top panel) and actin (bottom panel) in primary trophoblasts isolated from three different placentas. Numbers above represent fold difference between band intensities, analyzed by densitometry.

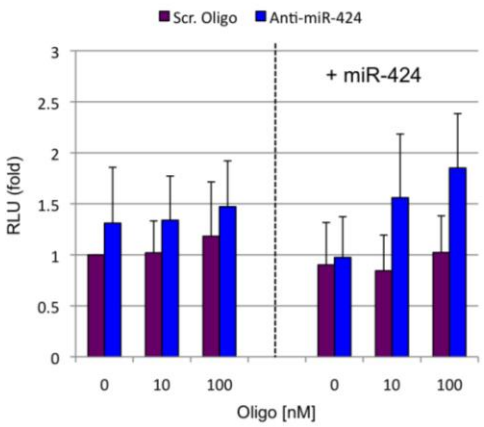

Fig. 2: Knockdown of miR-424 activity release silencing of FGFR1 reporter. HTR8/SV cells were transfected with the FGFR1 3'UTR reporter and an anti-miR-424 inhibitor or a scrambled oligonucleotide control (Scr. Oligo). Relative luciferase unit (RLU) activity was determined 48 h later. Data represent the mean of three independent experiments, performed in duplicate.

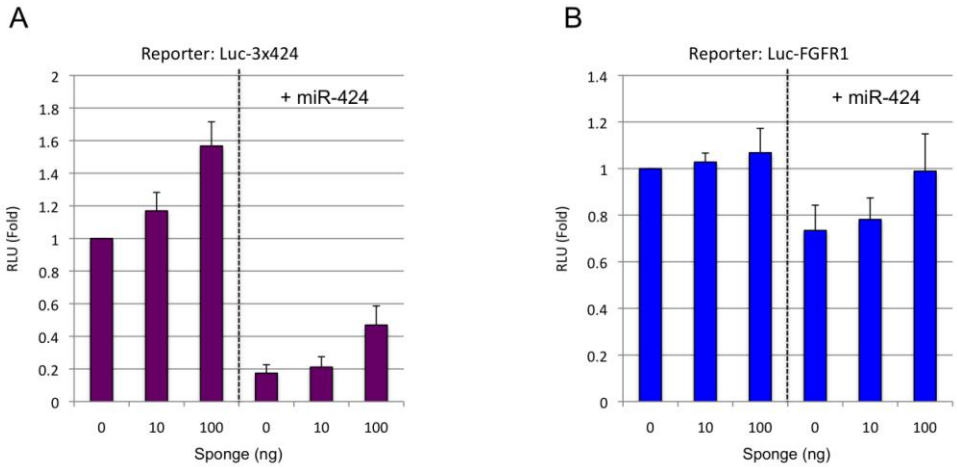

Fig. 3: Effect of the miRNA sponge on the activity of miR-424-mediated silencing of a luciferase reporter. HTR8/SV cells were transfected with a miR-424 sensor construct (A) or the FGFR1 3'UTR reporter (B) along with various amount of a plasmid expressing the miR-424 sponge. Relative luciferase unit (RLU) activity was determined 48 h later. Data represent the mean of three independent experiments, performed in duplicate.

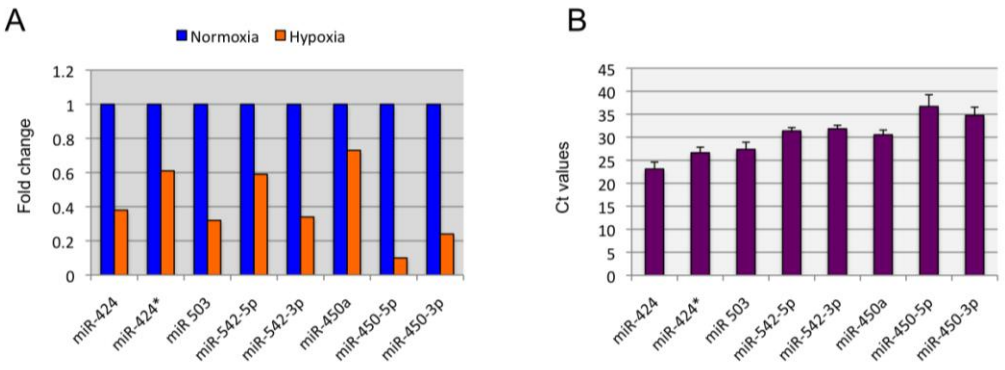

Fig. 4: Analysis of miR-424 cluster expression by real-time PCR. A) Downregulation of miR-424 cluster in hypoxia. Primary trophoblasts were cultured for 48 h in normoxia (20% O2) or hypoxia (1% O2). Expression level of individual miRNA was determined by real-time PCR using the miScript PCR System (Qiagen) and normalized with RNU6B. ΔΔCt method was used to analyse RT–qPCR data. Bars represent the mean value of four experiments. B) Relative expression levels of the different miRNA species from the miR-424 cluster. Bars represent the mean Ct value of four experiments.

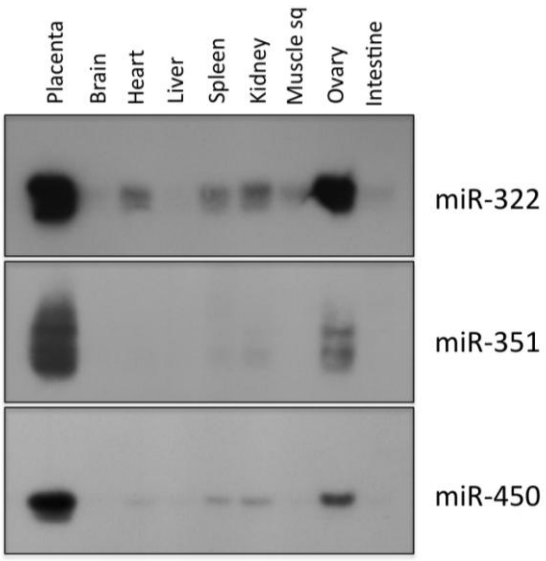

Fig. 5: Northern blot analysis of miR-424 miRNA cluster member expression in mouse tissues. Twenty micrograms of total RNAs were resolved on 15% denaturing poly-acrylamide gels, and transferred to nylon membranes. The blots were hybridized with ^{32}P-labeled probe complementary to the miRNAs indicated.

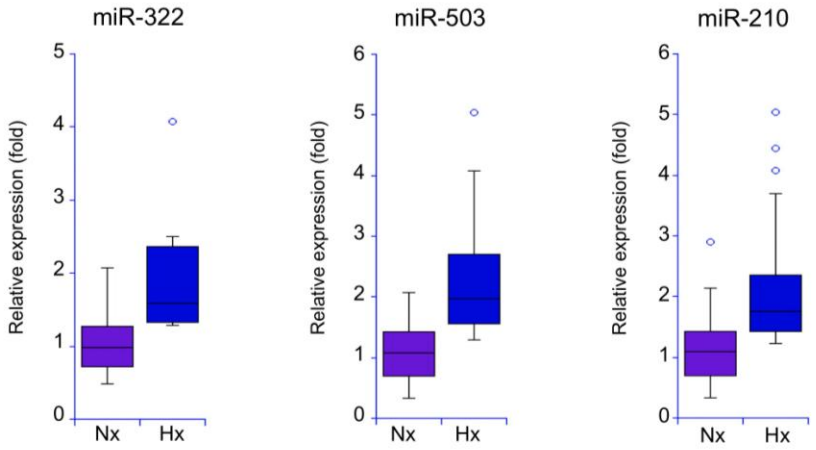

Fig. 6: Box plot comparing the expression of two miR-424 cluster members and miR-210 in placentas of pregnant mice exposed to low oxygen (Hx, n=10) relative to mice housed in standard conditions (Nx, n=11). The bottom and the top of the box indicate the 25 and 75 percentiles, respectively; the line in the box indicates the median value, and the whiskers indicate the minimum and maximum data values.

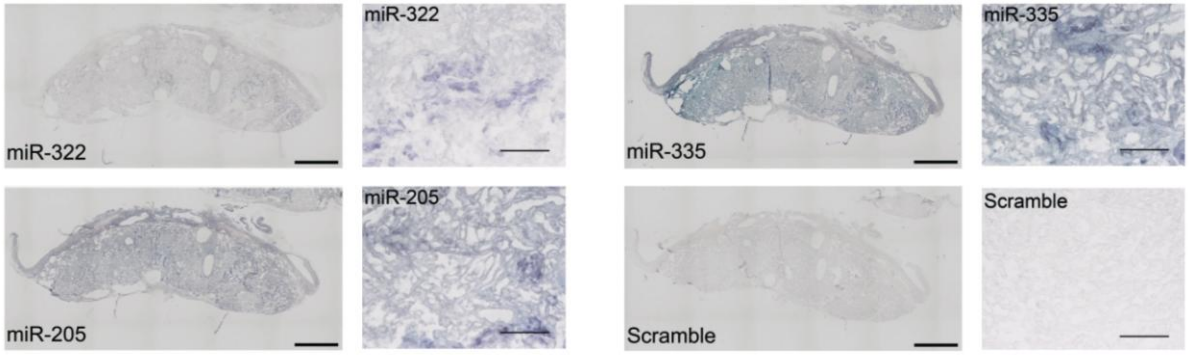

Fig. 7: *In situ* hybridization of miRNA in the mouse placenta. In situ hybridization analyses using 5' DIG-conjugated, LNA-modified antisense probes for miR-322, miR-205, and miR-335 and a scrambled oligonucleotide control. After washing the slides were incubated with alkaline phosphatase conjugated anti-DIG antibody and detected using BM Purple Substrate. For each miRNA we show a picture at low magnification (40x, scale bar = 1 mm) and high magnification (200x, scale bar = 100 μm).

Research Project 5: Project Title and Purpose

Epigenetic Analysis of Human Aneuploidy - Common chromosomal disorders resulting in live births include Down, Turner, Edwards and Klinefelter Syndromes. Although our knowledge of human aneuploidy has improved, there are still many gaps in our understanding of the mechanisms by which an altered number of chromosomes can lead to a specific disease phenotype. One area that has not been previously explored is the effect of aneuploidy on DNA methylation patterns. This is significant because appropriate DNA methylation is known to play a central role in gene regulation and normal homeostasis. This pilot project will therefore characterize genome-wide DNA methylation patterns in normal pregnancies and compare these to aneuploid pregnancies. A practical outcome of this work will be the identification of potential diagnostic biomarkers of human aneuploidy.

Duration of Project

1/1/2010 - 12/31/2010

Project Overview

DNA methylation is emerging as a key component of a broad repertoire of epigenetic mechanisms by which normal genome function and balanced homeostasis are maintained. However, we have only a limited understanding of the global organization of DNA methylation patterns and how they impact on gene regulation. DNA methylation patterns are highly tissue specific and are carefully organized and distributed across the genome in a fashion that is tightly regulated. We are interested in the consequences of an aneuploid state on the patterning of the DNA methylome and the possibility that global organization of DNA methylation is disrupted by the presence of an extra chromosome such as in trisomy 21. In addition to our interest in the biological basis of DNA methylation, we also hypothesize that the identification of DNA methylation patterns that are specific to aneuploidy may drive developments in fetal diagnostics via the discovery of biomarkers for the selective amplification of placental DNA from maternal plasma. Such markers could be exploited for the selective amplification of the fetal genome from maternal plasma DNA and the subsequent non-invasive diagnosis of fetal aneuploidy. Similar approaches have generated great excitement because definitive prenatal diagnosis of aneuploidy is currently performed using chorionic villus sampling (CVS) or amniocentesis. These are invasive, expensive and somewhat risky approaches that must be performed by experienced clinicians and are generally only offered to expectant mothers considered to be at elevated risk of carrying a genetically abnormal fetus. The guiding hypothesis of this project is that DNA methylation patterns in the placental villus of aneuploid pregnancies are markedly different than those of their normal euploid counterparts. Therefore, our primary aim is the comprehensive characterization of the placental DNA methylome in cells derived from chorionic villus samples obtained at the beginning of the first trimester from euploid and aneuploid pregnancies. To achieve this goal we will use a high-throughput microarray-based approach to compare methylation at approximately 27,000 CpG dinucleotides in genomic DNA isolated from CVS tissue and (cells cultured from these tissues) of approximately 24 aneuploid pregnancies and 24 normal controls. This approach will identify regions of DNA that are differentially methylated between these tissues on a genome wide scale. This information will serve as a foundation for

both the future development of non-invasive tests for fetal diagnosis and the development of our understanding of how aneuploidy affects the structure of the DNA methylome.

Principal Investigator

David G. Peters, PhD
Associate Professor
University of Pittsburgh
Magee-Womens Research Institute
204 Craft Avenue
Pittsburgh, PA 15213

Other Participating Researchers

Patricia Shaw, BS - employed by University of Pittsburgh Medical Center
Tianjiao Chu, PhD - employed by University of Pittsburgh

Expected Research Outcomes and Benefits

Major outcomes of this project will be the identification of regions of the human genome that are methylated in normal CVS tissues and the identification of locations at which these methylation marks are altered in samples from normal and aneuploid pregnancies. This information will provide insight into the biological significance of DNA methylation in these cells in a genome wide fashion and will develop our understanding of the epigenetic consequences of an altered number of chromosomes. Furthermore, these insights will identify regions of the genome where DNA methylation is altered in specific diseases such as Down, Turner, Edwards and Klinefelter Syndromes. There is currently great interest in the development of non-invasive diagnostic tests for fetal genetic disease that rely upon the analysis of cell free DNA obtained from maternal plasma. Such DNA samples contain detectable amounts of DNA derived from the placenta that can be used to genotype the fetus in a non-invasive fashion. One of the challenges in this field is distinguishing maternally inherited fetal alleles from identical endogenous maternal DNA. One approach to overcoming this barrier is to exploit unique placental DNA methylation patterns. Therefore, the differentially methylated regions we identify may provide us with methylation based diagnostic markers for the early detection of fetal aneuploidy using DNA obtained from maternal plasma. Such biomarkers would be defined by their ability to distinguish between normal and aneuploid fetuses. The development of such markers into routine clinical tests could enable the accurate diagnosis of fetal genetic disease during early gestation using DNA derived from maternal plasma samples. Such an approach would largely remove the requirement for invasive methods of diagnosis such as CVS or amniocentesis. In summary, this research project will greatly improve our understanding of DNA methylation in the context of aneuploidy and could lead to the development of noninvasive tests for the accurate diagnosis of related fetal genetic diseases in expectant mothers.

Summary of Research Completed

In the first six month period of this award, we focused on generating high density microarray

data to identify differentially methylated regions that exist between karyotypically normal and aneuploid CVS and cultured CVS tissue samples. These efforts yielded a significant amount of data. During the second six month reporting period, we have expanded upon our initial findings by exploring the validity of the microarray data and attempting to confirm DNA methylation differences we identified by the microarray analysis.

While preparing to expand upon our initial microarray findings, we were simultaneously carrying out a parallel study in which we are attempting to identify DNA methylation differences between gestational age-matched placental tissues obtained at delivery from normal mothers and mothers with preeclampsia. Preeclampsia is a physiological disorder of pregnancy in which high blood pressure and protein in the urine develop after the 20th week (late 2nd or 3rd trimester) of pregnancy. In this related study, like the current study, we used the Humanmethylation27 microarray platform. Interestingly we discovered that the 48 microarray data sets (derived from 24 normal and 24 diseased placental tissues) could be easily distinguished on the basis of fetal gender. Specifically, when we performed unsupervised hierarchical clustering on these samples, we identified two major clusters of samples. Regardless of disease state these were distinguished completely by fetal gender. Therefore, we conclude that fetal gender is an extremely strong signal in the context of DNA methylation. In light of this discovery, we re-analyzed our trisomy 21 microarray data. In this analysis we considered normal and trisomy 21 CVS samples from only female pregnancies or male pregnancies. The top twenty genes identified in this analysis for each fetal gender are presented in Table 1A (female) and 1B (male). Interestingly there were a significantly larger number of CpG loci identified in the samples from female pregnancies than male pregnancies. In fact we identified 301 loci that reached statistical significance when comparing normal versus trisomy 21 in the female tissues and only 25 in the male tissues.

Regardless of our method of data analysis, one characteristic of our microarray data is that, while differences between cultured and uncultured CVS samples are profound, differences between normal and trisomy 21 samples within either the cultured or uncultured sample groups were more subtle. Despite this apparent lack of a major distinction, we identified DNA methylation differences at CpG loci that were statistically significant between normal and aneuploid tissues (Table 1A and 1B) and we therefore attempted to confirm these using the Epityper platform marketed by Sequenom. This is a mass spectrometry based system that can detect mass differences between DNA fragments of different sequence. In this assay, purified DNA from a given sample is subjected to treatment with bisulphite. This results in the conversion of cytosine residues to uracil but leaves 5-methylcytosine residues unaffected. Thus, bisulphite treatment introduces specific changes in the DNA sequence that depend on the methylation status of individual cytosine residues, yielding single- nucleotide resolution information about the methylation status of a segment of DNA. It is this information that is detected during the mass spectrometry analysis.

For the Epityper analysis we focused on the CpG loci listed in Table 2. These were all genes that were identified as being differentially methylated in normal versus aneuploid uncultured CVS tissues. We focused on the uncultured samples because of the marked differences previously identified between cultured and uncultured samples, implying that methylation signatures are modified during cell culture. We felt that the uncultured molecular phenotype was therefore more biologically relevant than its cultured cell counterpart.

Although the primary microarray data generally identified only one specific CpG locus per gene of interest, the Epityper method is able to assay DNA methylation levels at multiple CpG loci within the surrounding genomic region. This region is specified by the length/location of the PCR fragment that is amplified following bisulphite conversion of DNA prior to mass spectrometry. The Epityper data corresponding to the sentinel CpG loci, which are those previously identified by the microarray analysis, are presented in Table 2. As can be seen in Table 2, the Epityper data, in general, do not support the findings of the microarray experiments in that CpG loci identified as differentially methylated in the latter are not corroborated by the former. This was true not only with respect to the sentinel CpG site but also the many other adjacent CpG loci that we co-amplified and therefore co-analyzed by the Epityper analysis (not shown).

The lack of corroboration between the two assay platforms is troubling. It is of course possible that the genes identified by the microarray experiments are not genuinely differentially methylated and are therefore false positive results. In any experimental system that contains relatively few replicates and thousands of data points there are bound to be some false positives and false negative results. However, we have previously performed large numbers of both Humanmethylation27 microarray and Epityper experiments and we have found that the data generally agree. It should be noted however that the majority of our experience with these platforms has been focused on the analysis of distinct cell or tissue types rather than normal and abnormal samples from the same anatomical tissue source. In such comparisons it is easy to find differences in DNA methylation that are very large.

One question that arises, with respect to the assay platform, is whether the Humanmethylation27 microarrays are of high enough density to collect information at relevant loci. This is because, although many thousands of genes are represented on the microarray, there are very few probes that are present per gene. We know from previous studies in our lab that DNA methylation levels can change quite dramatically in a spatial context along the chromosome. Therefore it is conceivable that the assay platform is missing significant differences in DNA methylation by not providing enough gene-specific sensitivity.

Before performing any more experiments with our valuable trisomy 21 tissue samples, we therefore sought to develop a new technology that, ideally, would be able to assay DNA methylation levels at far more loci and at much higher accuracy. Our goal was to combine a previously used method based on a custom microarray platform developed in our lab with next generation DNA sequencing. In our previous microarray method we had generated libraries of methylated and unmethylated DNA fragments using the restriction enzyme isoschizomers HpaII and MspI. These enzymes both cleave at CCGG core recognition sequences but the former will only cut when the DNA is unmethylated and is therefore blocked when it is methylated. In contrast MspI cuts regardless of whether the CCGG site is methylated. By using one or the other enzyme to cut each of two aliquots of the same DNA, it is possible to compare the restriction fragments to identify differentially methylated sequences. In our previous microarray method we combined this isoschizomer profiling approach with the addition of a second restriction enzyme called TspR1 in conjunction with an Exonuclease III digestion step. This enzyme generates 9bp single stranded DNA overhangs that are resistant to cleavage by Exonuclease III. However, HpaII or MspI generate 2bp over-hangs that are sensitive to Exonuclease III cleavage.

Therefore if a TspR1 digested fragment is cleaved internally by HpaII or MspI then it will be lost from the library. Using this approach one is able to generate a methylated CCGG site-enriched fragment library when digestion with HpaII takes place. Libraries digested with MspI and sham-digested libraries serve as positive and negative controls respectively. In our new approach, the resulting DNA fragment libraries are used as substrates for the construction of DNA sequencing libraries using Illumina next generation sequencing chemistry. Using this approach we have generated first proof of concept by preparing TspR1 fragment libraries of normal CVS sample in duplicate and carrying out DNA sequencing. A schematic diagram highlighting this method is presented in Figure 1 and preliminary DNA sequencing data is shown in Table 3.

SUMMARY AND CONCLUSIONS

In summary we were unable to confirm aneuploidy-specific differences identified by microarray using the Epityper method despite controlling for fetal gender, which we have found to have a profound influence on genomic DNA methylation patterns. Because of this lack of agreement between primary microarray data and gene specific follow up analysis by mass spectrometry, we speculated that the microarray platform is not sensitive enough to detect subtle differences in DNA methylation on a genome wide scale. Because of the high value of our affected samples we elected not to perform any more experiments with these until we have further refined our analytical tools. We therefore developed a novel method for genome wide DNA methylation analysis based upon high throughput DNA sequencing. Preliminary data suggests that this method may have significant potential for the analysis of disease-specific changes in DNA methylation at high resolution on a genome wide scale.

Table 1A. Humanmethylation27 Infinium microaray data. Top twenty differentially methylated CpG sites identified in comparison between uncultured trisomy 21 CV samples compared to uncultured normal samples (female fetus). "Mean Norm" and "Mean T21" are mean of the proportion of methylated CpGs at the specified locus (probe ID).

Probe ID	adjPvalue	Mean Norm	Mean T21	Gene
cg00090147	0	0.298	0.615	GATA4
cg00363813	0	0.193	0.515	HOM-TES-103
cg01259619	0	0.022	0.337	ITPKB
cg01942127	0	0.170	0.429	CACNA1D
cg02919422	0	0.084	0.266	SOX17
cg06509239	0	0.055	0.349	OSR1
cg06821993	0	0.070	0.342	CSMD3
cg08062469	0	0.042	0.105	SPAG5
cg08145590	0	0.054	0.145	C3orf15
cg09587549	0	0.085	0.402	PYCARD
cg09874752	0	0.043	0.167	SFRP5
cg10976172	0	0.263	0.582	FLJ32130
cg14015044	0	0.034	0.215	TNFRSF10C
cg15239123	0	0.060	0.366	SMOC1
cg15755084	0	0.043	0.275	MSX1
cg17049328	0	0.518	0.255	GHRH
cg17665193	0	0.109	0.309	GAD2
cg19011603	0	0.135	0.315	RP11-311P8.3
cg19215261	0	0.790	0.938	SLC25A2
cg20358834	0	0.052	0.403	LRFN4

Table 1B. Humanmethylation27 Infinium microaray data. Top twenty differentially methylated CpG sites identified in comparison between uncultured trisomy 21 CV samples compared to uncultured normal samples (male fetus). "Mean Norm" and "Mean T21" are mean of the proportion of methylated CpGs at the specified locus (probe ID).

Probe ID	adjPvalue	Mean Norm	Mean T21	SYMBOL
cg01980637	0	0.035	0.492	PER1
cg02566518	0	0.059	0.388	FUT11
cg06819200	0	0.014	0.336	ECE1
cg14617642	0	0.029	0.564	H2AFY2
cg17163751	0	0.034	0.426	H2AFY2
cg22836229	0	0.053	0.423	EFCAB1
cg24473633	0	0.273	0.028	DENND3
cg20322876	0.018	0.460	0.043	FLJ45803
cg16545079	0.020	0.036	0.215	PER1
cg13055278	0.024	0.057	0.226	ID2
cg20166532	0.024	0.193	0.041	EDG1
cg01366419	0.027	0.063	0.299	WBSCR17
cg21561173	0.028	0.069	0.383	C21orf81
cg01204439	0.029	0.287	0.063	TPK1
cg00958560	0.029	0.559	0.229	FLJ46481
cg25760229	0.029	0.061	0.260	CACNA1H
cg17830308	0.029	0.103	0.368	NEUROG1
cg20540428	0.029	0.176	0.491	PPP4R2
cg23367478	0.032	0.159	0.024	PDE3A
cg08731300	0.032	0.046	0.174	FZD8
cg27225570	0.032	0.059	0.225	DUSP15
cg04786857	0.032	0.032	0.165	SPDY1
cg20450764	0.044	0.125	0.349	TSPAN7
cg16509658	0.045	0.089	0.292	GABRB2
cg14221171	0.047	0.282	0.548	TAC1

Table 2. Epityper data for female only uncultured fresh CVS samples. Only sentinel CpG sites, initially identified as significant in the microarray data are shown

Probe ID	Gene	Norm mean	T21.mean	pval. wilcoxon	adj.pval. wilcoxon
cg07922606	HIST1H3E	0.08	0.28	0.009	0.235
cg21296230	GREM1	0.44	0.46	0.683	0.830
cg11830061	INSL6	0.29	0.38	0.268	0.521
cg08032971	DMBX1	0.36	0.45	0.104	0.327
cg26186727	NETO1	0.16	0.21	0.103	0.327
cg08062469	SPAG5	0.06	0.09	0.322	0.582
cg10976172	FLJ32130	0.23	0.37	0.104	0.327
cg20723355	FBXO39	0.11	0.20	0.102	0.327

Table 3. Summary data for DNA sequencing of libraries prepared using the new TspR1 method. S1 and S2 are duplicates of HpaII digested DNA. S3 and S4 are duplicates of MspI digested DNA. S5 and S6 are duplicates of sham digested DNA.

Library	Enzyme	Original reads	Matched reads	Distinct matched reads	Matched/ Original	Distinct matched/ Matched
s1	Sham	11386931	6656388	1381483	0.58	0.21
s2	Sham	14111299	10260793	1923606	0.73	0.19
s5	HpaII	23080529	16131370	480194	0.70	0.03
s6	HpaII	24498779	18290725	1137790	0.75	0.06
s7	MspI	9011591	3264193	1026826	0.36	0.31
s8	MspI	9425937	5228484	1302572	0.55	0.25

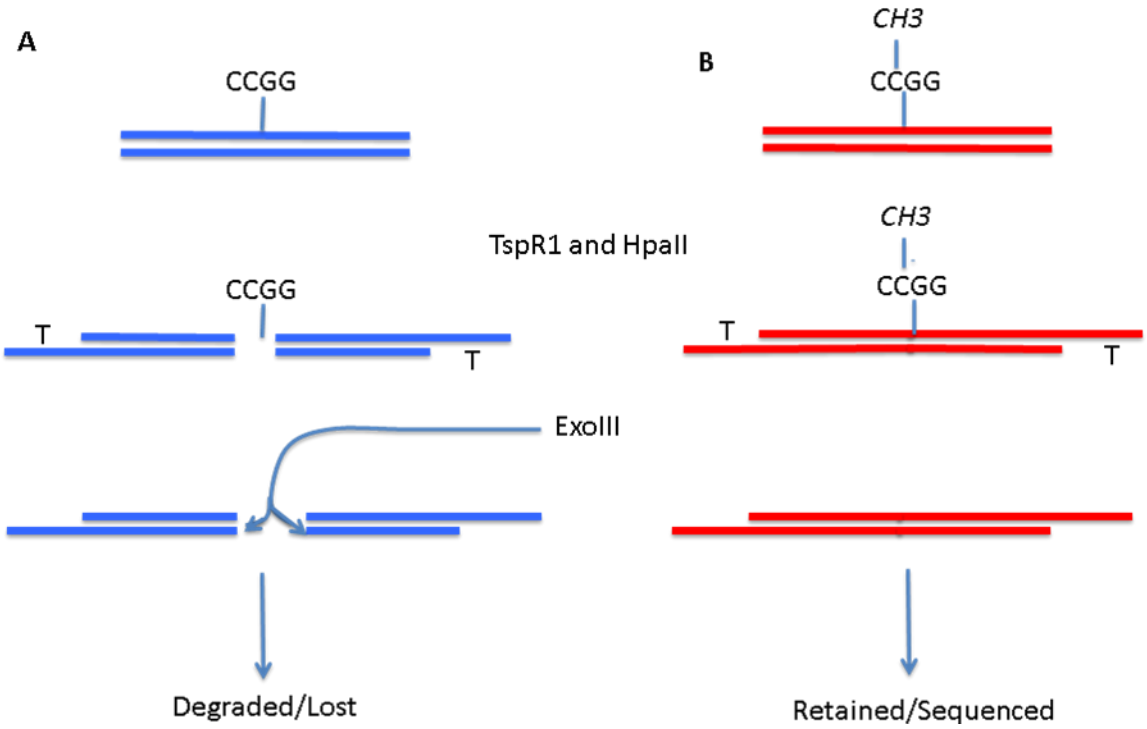

Figure 1**.** Schematic diagram of TspR1 method for enrichment and sequencing of methylated DNA fragment libraries. Panel A (left/blue) depicts an unmethylated DNA fragment which is cleaved by both TspR1 (yielding 9 base single stranded overhanging ends [“T”]) and HpaII. Because the CCGG site is not methylated, HpaII can cut. The resulting 2 base overhangs are sensitive to digestion by Exonuclease III and the fragment is lost from the library. In contrast, an identical sequence that is methylated will be resistant to HpaII cleavage. 9 base single stranded TspR1 digested ends will protect the fragment from digestion by Exonuclease III and the fragment will remain in the library and will later be sequenced.

Research Project 6: Project Title and Purpose

Antigen Expression and Adaptive Immunity in Human Endometriosis and Endometriosis-Related Ovarian Cancers - Ovarian cancer most often presents as advanced disease and survival at 5 years is very low. We postulate that identification of precursor lesions would allow for timely detection of early ovarian cancer and will ultimately improve survival. To date, the only precursor lesion reported in ovarian cancer is endometriosis, a common disease which can affect up to 10% of reproductive-age women. However, the major pathogenesis mechanisms are not well understood in either ovarian cancer or endometriosis. One common denominator of these two clinical entities is chronic inflammation, given by the interaction of cancer cell-intrinsic factors and the host immune system. We postulate that a better understanding of the role of the adaptive immune system in endometriosis could potentially contribute to the design of vaccines used for ovarian cancer prevention rather than therapy.

Duration of Project

1/1/2010 - 12/31/2010

Project Overview

An intact immune system is capable of surveying for cancerous or even precancerous lesions and eradicating them before they become clinically significant. This process is known as immunosurveillance and relies on the function of highly specialized immune cells and their secreted molecules (called adaptive immunity). The immune mechanisms (and their failures) although studied in cancer, are much less understood in premalignancy, including endometriosis. We postulate that in the context of chronic inflammation, the immune surveillance may in fact contribute toward lesion development (invasion, angiogenesis etc) and malignant transformation. We propose here to characterize the interactions between the epithelial cells and immune cells in the microenvironment, in endometriosis and ovarian cancer. Some of these interactions are antigen-specific, in response to protein antigens expressed by the epithelial cells during disease progression. One such antigen is MUC1, a well known oncoprotein and tumor-associated antigen widely expressed in all types of ovarian tumors and present in endometriosis. Our previous studies in MUC1 Tg mice with conditional Kras mutations (MUC1Kras mice) progressing to endometriosis-like lesions illustrate a progressive increasing in MUC1 expression and T cell dysfunction suggestive of Th2/Treg bias. Ovarian tumor-bearing (MUC1KrasPTEN) triple transgenic mice also show presence of Th17 cells in advanced disease. Based on these results, we propose here the following aims:

Specific Aim 1: To identify the mechanisms of immune surveillance in peripheral blood and lesion microenvironment in human endometriosis and ovarian cancer. We will explore T and B-cell mediated immunity and characterize the immune balance between CD4+ T cell subsets, specifically Treg and Th17 subsets, in human endometriotic lesions. As controls we will use patients with malignancy (cancer control patients) and patients with benign lesions (physiologic cysts- benign control patients). We will use several platforms to profile antigen expression and immunity, using immunohistochemistry, flow cytometry and quantitative real time PCR arrays.

Specific Aim 2: To identify MUC1 roles in ovarian carcinogenesis. For this aim we will use 2 categories of transgenic mice, both progressing to de novo ovarian tumors: 1. triple transgenic (Tg) MUC1KrasPTEN mice which develop human MUC1-expressing ovarian tumors and 2. double Tg KrasPTEN mice, which develop MUC1-negative ovarian tumors. These mice will allow us to characterize phenotypic differences due to human MUC1 and identify potential new therapeutic targets.

Principal Investigator

Anda M Vlad, MD, PhD
Assistant Professor
University of Pittsburgh
Magee Women's Research Institute
204 Craft Ave., B403
Pittsburgh PA 15213

Other Participating Researchers

Raluca Budiu, PhD - employed by University of Pittsburgh
Joan Brozick, BS - employed by University of Pittsburgh Medical Center

Expected Research Outcomes and Benefits

Immediate significance: Our studies will further our understanding on the role of the immune system in disease pathogenesis in endometriosis and it will provide insight on the expression of MUC1 antigen in endometriosis.

Long-term impact: Results from these studies will hopefully provide the basis for the next generation MUC1 vaccines and immune biologics, targeting prevention rather than cancer treatment.

Many clinicians and translational scientists currently allocate substantial efforts to the design and implementation of vaccines and immune biologics as adjuvant therapy in late stage cancer patients. Most often, the patients are terminally ill, and the disease is resistant to standard therapy. Not surprisingly, the immune system in these patients is exhausted and unable to respond to its full potential given the disease burden. On the other hand, however, patients with long-lasting, chronic premalignant disease (like endometriosis) are generally younger and better candidates for vaccines or immune biologics. Studies presented here will hopefully provide a first step toward the design of preventive vaccines.

Summary of Research Completed

During the second half of the funding period, the PI has successfully completed the proposed specific aims, as set forth in the original grant application. Details of our results are described below.

Specific Aim 1: To identify the mechanisms of immune surveillance in peripheral blood and lesion microenvironment in human endometriosis and ovarian cancer.

Our hypothesis is that adaptive immune cells, particularly T cells and their secreted factors could functionally contribute toward lesion development (i.e., invasion, oxygenation, angiogenesis, etc.) in endometriosis and may potentially drive ovarian carcinogenesis. To test this hypothesis, we proposed to explore the tissue microenvironment in endometriosis and to profile the immune balance between CD4+ T cell subsets using immunohistochemistry, flow cytometry and quantitative real time PCR arrays.

Specimen accrual and tissue bank resources.
We collected and evaluated during this granting period, a total of n=30 ovarian endometriotic lesions and associated fluids, n=25 endometriosis-related cancers (tissue biopsies, blood, ascites, etc.) and n=15 normal controls (tissue, peripheral blood).

The specimens were acquired from Health Science Tissue Bank at Magee-Women's Hospital and the Gynecologic Specimen Bank, according to approved IRB exempt protocols.
All tissue and blood specimens were processed within 2 hours from harvesting.
The PBMCs were fractionated from plasma and cryopreserved until ready to use. The tissue was processed for formalin fixation and paraffin embedding.

Immunohistochemistry (IHC) and quantitation of tissue T cell infiltrates.
We have completed the IHC staining for four immune markers (CD3, CD4, CD8, and FoxP3) on all formalin fixed and paraffin embedded (FFPE) tissue sections obtained from women with endometriosis and endometriosis-related ovarian cancer. We have also performed staining on all available eutopic endometrium specimens for these patients.

The observed IHC staining pattern for CD3, CD4, FOXP3 T cell infiltrates was described in the previous report. In the second half we digitally quantified the staining results from all cases (n= 67 total), using the NIS Elements AR software (Nikon, version 3.01) and completed the statistical analysis. Our results show significantly lower total CD3 T cell as well as CD8 T cells in epithelial ovarian cancer (EOC) versus endometriosis. Furthermore, the CD3:Foxp3 and CD8:Foxp3 ratios were significantly higher in endometriosis than in endometriosis-associated ovarian cancer (EAOC). These findings demonstrate that in contrast to premalignancy, the epithelial lesions in cancer contain fewer CD3 T cells and CD8 T cells and the effector –to – suppressor cells is much lower in cancer (Fig.1). These results suggest that although CD8 T cells and FOXP3+ regulatory T cells (Tregs) are present at any stage (normal, premalignant or malignant), CD8 T cell effectors are drastically affected during progression to malignancy, which tips the balance into the favor of immune suppression.

RNA extraction and qRT-PCR arrays.
To further explore the tissue microenvironment in endometriosis and ovarian cancer and to profile the immune balance between CD4+ T cell subsets, we used quantitative real time PCR arrays.
Patient categories: We extracted RNA from 3 patient categories: endometriosis, endometriosis-related ovarian cancer and normal controls.

Specimens collected: From each patient, we extracted RNA from FFPE tissue (ovarian tumor, endometriosis lesion, normal endometrium) and peripheral blood mononuclear cells (PBMC). *Quantitative real-time RT-PCR profiler arrays*: We used two sets of genes, one focused on immune cell differentiation (immune profiler array) and the other focused on MUC1 antigen and MUC1-driven pathway (MUC1 profiler array).

We identified a significant number of potential immune biomarkers of disease (Fig 2 and 3). Many of the significant RNA changes observed are currently confirmed at the protein level in both peripheral tissue as well as circulating blood.

Specific Aim 2: To identify MUC1 roles in ovarian carcinogenesis.
Rationale and hypothesis. For this aim we used 2 categories of transgenic mice, both progressing to de novo ovarian tumors: 1. triple transgenic (Tg) MUC1KrasPTEN mice which develop human MUC1-expressing ovarian tumors and 2. double Tg KrasPTEN mice which develop MUC1-negative ovarian tumors. Since the only difference in these two sets of mice was the presence (or absence) of MUC1 antigen, any observed phenotypic difference would be due to MUC1 roles in ovarian cancer pathogenesis.

Results.
We have carefully profiled the characteristics of tumors from triple (n=10) versus double (n=13) Tg mice. Despite histomorphologic similarities (ovarian tumors with endometrioid histology in both), we observed several contrasting features, summarized in more detail in the final report.

Using a scoring system based on the number of anatomical location of metastases at necropsy, we observed that the MUC1-expressing tumors metastasize more widely in the peritoneal cavity. The triple Tg mice had an average of 2.6 metastatic sites versus 1.4 in double Tg mice (p=0.03). Furthermore, the primary (ovarian) tumors seemed smaller in MKP mice than KP mice (tumor score of 2.1 and 2.7, respectively p=0.08) and had the tendency to be accompanied more often by ascites (90% and 54%, respectively p=0.09), although statistical significance for these two findings was not reached.

We detected significant down-regulation of cadherin 11 (Cdh-11) in MUC1-expressing versus MUC1 negative mouse tumors at both RNA (not shown) and protein levels Cadherins normally mediate adherens junctions and maintain epithelial morphogenesis. They also act as tumor suppressor genes and are implicated in a wide array of functions, including signal transduction (through growth factors), inflammation and metastasis, mainly via beta-catenin/Wnt pathway.

Identified as a tumor suppressor in retinoblastoma and associated with metastasis to the bone in prostate cancer, the complete roles of Cdh-11 in loco-regional tumor progression and invasion are not fully understood.

In line with the RNA results, the IHC staining of tumors with a mouse Cdh-11 antibody revealed lower Cdh-11 protein expression in triple Tg mice. We also confirmed this inverse MUC1-Cdh-11 correlation *in vitro*, using the MUC1-tranfected mouse IG10 ovarian cancer cells (IG10-MUC1). We found significant down-regulation of Cdh-11 at both RNA (not shown) and protein levels in IG10-MUC1 cells versus parental IG10 cells (Fig. 4).

Collectively, these results from triple and double Tg mice with ovarian tumors suggest that although MUC1 is not required for ovarian carcinogenesis, when both Kras and Pten/PI3k pathways are active, up-regulation of human MUC1 in the ovarian surface epithelium (OSE) may contribute to increased loco-regional tumor metastasis and epithelial-to-mesenchymal transition (EMT), potentially via Cdh-11 down-regulation. Furthermore, MUC1 positive tumors are accompanied by an increase in Treg accumulation in the spleen (Fig. 5), implicating MUC1 in loco-regional immune suppression. Additional details of our research results are included in the final report.

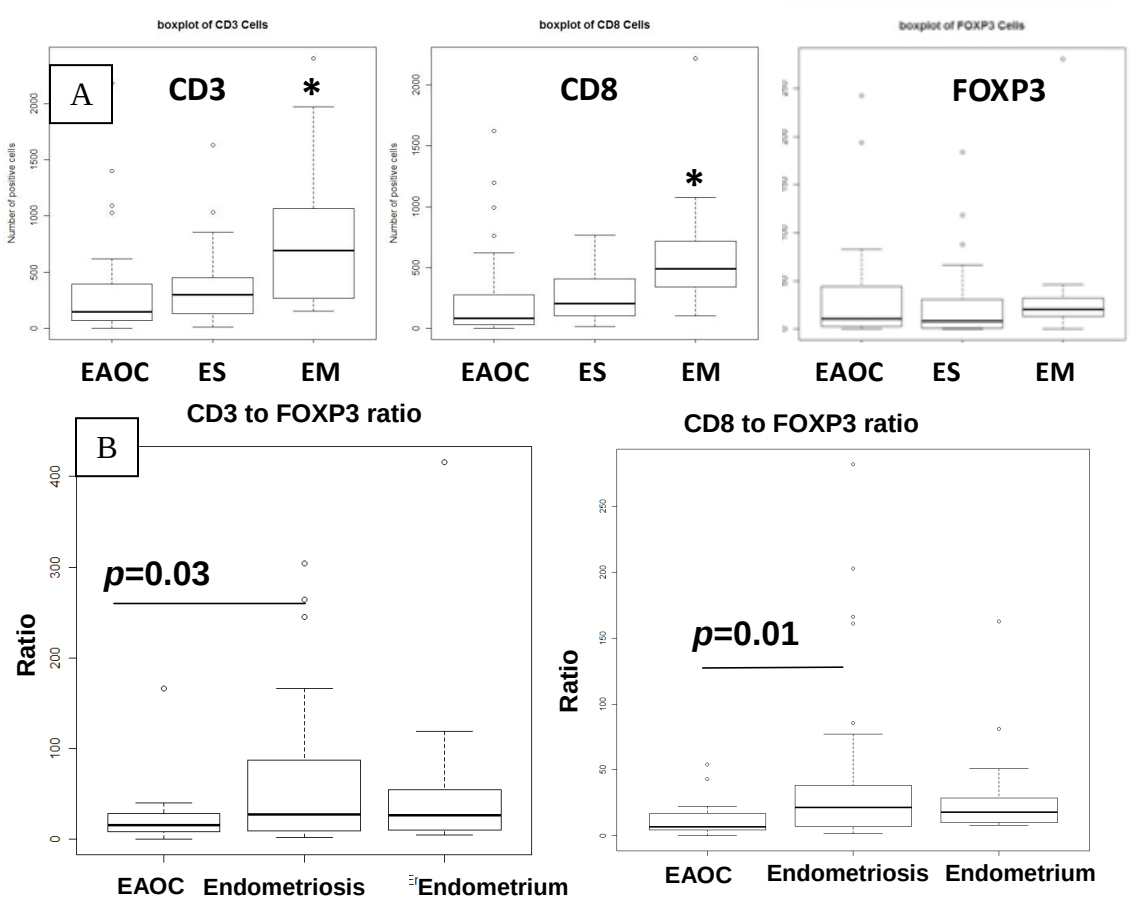

Fig.1. CD3, CD8 and Foxp3 immune marker staining measurements (A) and the ratios of CD3:Foxp3 and CD8:Foxp3 cells (B) were compared between groups using t-test and Wilcoxon rank-sum test. * p value <0.05, t test.

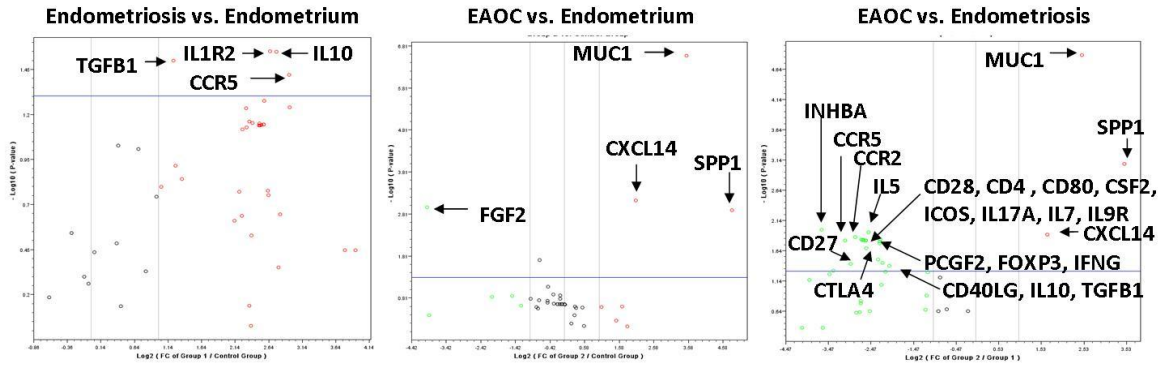

Fig. 2. Tissue Immune Gene Profiling in endometriosis (n=14), EAOC (n=10) and endometrium (n=9). Volcano plots showing differentially expressed genes (arrows). Up-regulated genes are shown in red and down-regulated genes in green.

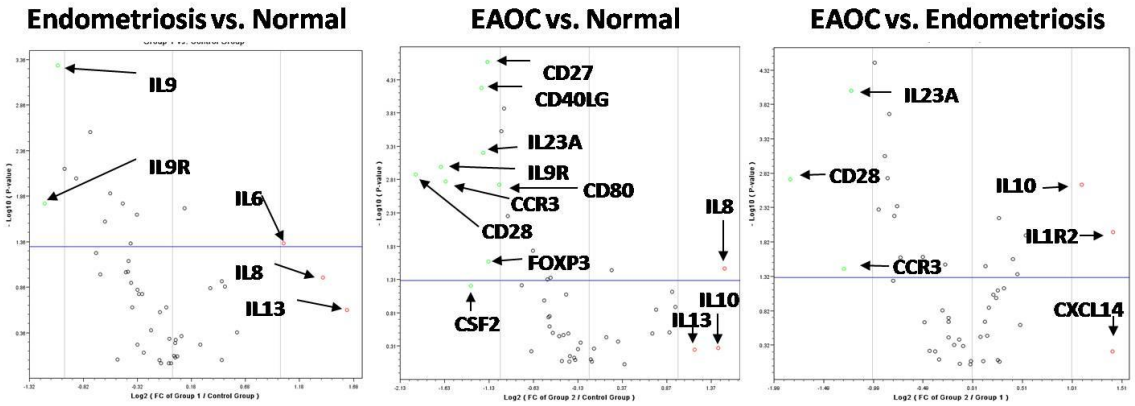

Fig. 3. Peripheral blood cells (PBMC) immune gene profiling. Differential expression of immune genes in endometriosis vs. normal (left) EAOC vs normal (middle) and EAOC vs. endometriosis. RNA was extracted from from PBMC of each patient. A 42 gene real-time PCR immune profiler array (Th1-Th2-Th3, SABiosciences), was used to monitor immune gene profiles. The data was analyzed using PCR Array data Analysis Web Portal (SABioscences), with a boundary of 2 fold change and a statistical significance of $p \leq 0.05$. Highlighted genes (arrows) show down-regulated (green) and up-regulated (red) genes.

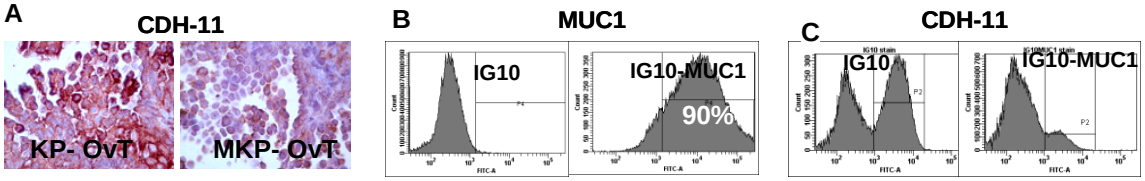

Fig. 4. Inverse MUC1-Cdh-11 correlation in ovarian tumors and cell lines. A: IHC staining of ovarian tumors (OvT) for mouse Cdh-11. B and C: Flow cytometry for cell surface MUC1 (B) and Cdh-11 (C) on mouse IG10 and MUC1-tranfected IG10-MUC1 cells.

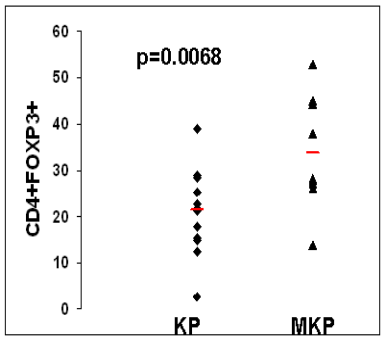

Fig. 5. Triple Tg (MKP) mice have increased Treg accumulation in the spleen, compared with double Tg (KP) mice with tumors. The splenocytes were phenotyped by multicolor flow cytometry using markers for CD3, CD4, CD25 and FOXP3. The percentages shown were of CD4FOXP3+ T cells. p=0.0068, Student's t test.

Research Project 7: Project Title and Purpose

The Impact of Age on the Nematode Germline - In human oocytes, defects in meiotic crossover exchanges are the most significant age related abnormality. Nevertheless, our understanding of the processes that control where and how many crossovers occur is not well understood. Furthermore, it is unclear how aging impinges on different crossover configurations to increase missegregation at increased maternal age. Our studies in the nematode *C. elegans* will use high resolution confocal imaging to identify changes in the germline chromatin structure during normal aging and will analyze how aging pathways influence these processes. These studies have the potential to identify genes and pathways that lead human aneuploidy and therefore may identify targets for therapeutic purposes.

Duration of Project

1/1/2010 - 12/31/2010

Project Overview

The goal of this research is to identify factors contributing to the age-related decline in fertility and the associated increase in trisomies. As women age, oocytes show problems in meiosis that lead to chromosomal nondisjunction (NDJ), including Turner and Down Syndromes. The majority of NDJ is due to defects in meiotic crossover recombination (CO). A growing body of literature places chromatin structure as a key determinant of CO formation. Thus changes in germline chromatin impact embryonic outcomes and through epigenetic inheritance, chromatin affects offspring fecundity. We will study age-related changes in germline chromatin in the model genetic system, the nematode *C. elegans* because there is strong conservation in aging pathways and in the meiotic process between worm and humans.

1) Characterize changes in germline chromatin during normal aging. Histone post-translational modifications and histone variant influence gene activity, DNA damage repair, and meiotic recombination and thus play a critical role in genome integrity. Because environment and age can modulate chromatin structure, we hypothesize that age-dependent changes in chromatin structure increase NDJ and predispose progeny to reproductive problems. We will characterize histone post-translational modifications and histone variants in the germlines of young and aged animals using immunofluorescence and high-resolution confocal imaging. These studies have

the potential of precisely describing how chromatin changes in the germline of aging animals and thus may reveal targets for reproductive therapies.
2) Identify molecular pathways controlling age-related changes in germline chromatin. Changes in chromatin structure are mediated by the histone modifying enzymes that catalyze the addition and removal of these marks. Chromatin structure is also influenced by endocrine signaling and environment which affect the expression and activity of these enzymes. In this aim, we will identify changes in expression of histone modifying enzymes during germline aging and associate these changes with specific modifications. We will also determine which of the aging pathways impinge on germline chromatin, by monitoring histone post-translational modifications and histone variants in longevity mutants. Initial efforts will focus on the characterization of *sir-2*, which has a direct role in chromatin modification and aging, and the insulin/IGF-1 signaling pathway, which affects resistance to germline tumors and reduces fecundity.

Principal Investigator

Judith L. Yanowitz, PhD
Assistant Professor
Magee-Womens Research Institute
204 Craft Ave, B705
Pittsburgh PA 15213

Other Participating Researchers

None

Expected Research Outcomes and Benefits

The ultimate goal of this work is to find conserved molecular pathways that inform our understanding of human infertility. Defining the genetic mechanisms that underlie defects in meiotic recombination and subsequent chromosome segregation is a critical step for understanding human reproductive aging. Chromatin organization is a major determinant of crossover regulation, influencing where and how many crossovers occur. Sex, age and temperature strongly influence the placement of crossovers along the chromosome by shifting the usage of chromosomal domains leading to the hypothesis that these factors influence crossover formation by altering germline chromatin. Our studies should identify specific histone post-translational modifications that are altered in aging animals and the aging pathways that are responsible for such changes. These findings have immediate applications for fertility research because drugs targeting either specific histone modifying enzymes and aging pathway components can be tested for their immediate effect on reproductive outcomes in the nematode. These results can then be used to inform studies in mammals, and ultimately the clinic. A second, potential outcome of these studies is the identification of potential targets for environmental toxicants within the germline. Aging pathways and stress pathways are intimately linked and many environmental toxins activate these pathways. Therefore, a greater understanding of germline targets of aging can inform our understanding of how stress and toxins act within the germline. The recent realization that bisphenol A, a commonly used

plasticizer, has severe germline phenotypes over multiple generations underscores the importance of our studies.

Summary of Research Completed

We have been screening for epigenetic changes in the germlines of aging worms to determine if changes in higher order DNA structure contribute to reproductive decline and aneuploidy. Over the last 6 months of this grant, we have extended our analyses of histone post-translational modifications (HPTMs) and histone variants over the course of reproductive life in the germlines of the nematode, *Caenorhabditis elegans*.

We performed more detailed analysis of HPTMs, analyzing sub-nuclear localization, pattern of distribution, and intensity in adult day 1 versus adult day 9 germlines. Consistent with our previous results, these studies failed to reveal differences in HPTMs between young and old animals (for examples, see Figure 1). Therefore, we conclude that gross changes in the epigenetic landscape are not a driving force of reproductive aging.

We did, however, observe that phosphorylation of histone H3Serine10 differed between young and old germlines (Figure 2). This modification is a hallmark of dividing cells, and it is observed in nuclei in the distal proliferative zone of the gonad, as well as in maturing oocytes, just prior to ovulation. In young germlines, we routinely saw between 2 and 10 nuclei within the mitotic zone that stained positive for this marker (average 7.4, N = 20 germlines). In aged worms, the number of nuclei that displayed intense staining was reduced to <1, but an increase in staining intensity (over background) was observed for all of the nuclei within this region (Figure 2). This result raises the possibility that a decrease in proliferative capacity of nuclei within the mitotic zone may directly promote reproductive senescence.

We next asked whether the *daf-2* or *sir-2* pathways extended reproductive lifespan, and if so, whether they directly controlled H3Serine10 phosphorylation. We did not observe an increase in reproductive lifespan in *sir-2.1* or *sir-2.3* mutant background. In both backgrounds, reproductive decline began on days 4-5 and worms were fully sterile by day 9-10. Given this result we did not observe any differences in H3Ser10 in these mutants.

In the *daf-2(e1370)* background, we found a slight, but measurable increase in reproductive span with some animals giving progeny up to 4 days beyond the wild type controls, consistent with recently published data. However, in this mutant background overall fertility was comprised with average brood sizes half that of wild type. Other *daf-2* alleles do not prolong reproduction: therefore, we were concerned that the effects on reproduction in the *e1370* background were due to a second site mutation in the stock. For that reason, initial efforts to outcross the stocks have been performed and are ongoing.

We wanted to extend our studies to the analysis of histone variants. We had previously tested antibodies to H2A.Z/Htz-1 and saw no differences between young and old tissue. Antibodies for other histone variants are not available, so instead we obtained histone::GFP transgenic lines and analyzed their expression in the germline. Even after outcrossing, none of these transgene lines expressed within the germ lineage. This is a common problem with *C. elegans* transgenes.

Protocols to produce low copy integrated transgenic lines are now available, but would have required a substantial investment of time and effort that were beyond the scope of this grant. Therefore, although we intended to test these histone variants for changes within the aging germ lineage, the lack of expression of transgenes sidelined these studies.

Although we did not observe changes in histone modifications using immunofluorescence, we cannot dismiss the possibility that biologically relevant changes are occurring that are too subtle to be detected using this procedure. Indeed mutation of the worm histone methyltransferase *spr-5* causes reproductive failure after many generations suggesting that small changes in the epigenetic landscape each generation can leading to severe consequences after many generations.

Therefore, we set out to develop an assay to test whether there are heritable epigenetic differences between young and old germ cells that ultimately impinge on fecundity. Unlike humans, the *C. elegans* germline is proliferative throughout adult life providing a continuous source of germ cells until the onset of senescence. The germline is organized in a spatial and temporal gradient, so that the first eggs laid (and the corresponding first larvae to hatch out) correspond to the first daughter cells of the germline stem cell population. Likewise, the last progeny produced correspond to the daughter cells produced after many cell divisions. Previous studies in *C. elegans* have suggested that there is a compromise in egg quality from older mothers (Luo et al. 2010). In humans, analysis of Icelandic populations has identified differences in the crossover landscape between the progeny of older mothers versus younger mothers (reviewed in Lynn et al. 2004).

Therefore, we asked whether we could observe differences in fecundity in lines bred from younger mothers to those bred from the older mothers. This experimental approach is shown in Figure 3a. We first tested this protocol in a sensitized genetic background: a strain carrying a mutation in *rfs-1*, a Rad-51 family protein required for replication fork progression. In the absence of *rfs-1*, sterility ensures after many generations due to the aberrant repair of replication fork errors leading to chromosomal abnormalities. In the inbred line from older mothers, we could detect chromosomal defects within 5 generations compared to 30-50 generations in young mothers (Figure 3b). Thus, this approach suggests that there are fundamental differences in the germline from old versus younger mothers. We also repeated this experiment with a mutation in *xnd-1*, a mutant that is required for meiotic crossover control and the modulation of histone H2A lysine 5 acetylation. After 5 generations of passage through an aged maternal germline, the majority of *xnd-1* animals were infertile, and the remainder were severely compromised in fertility as compared to those born of young mothers (Figure 3b). Thus, we have established that by carrying mutations through the aged germline, we can speed up the onset of reproductive decline that occurs in these populations. Since *xnd-1* shows defects in histone H2A acetylation, this validates this approach for the analysis of other histone modifying enzymes.

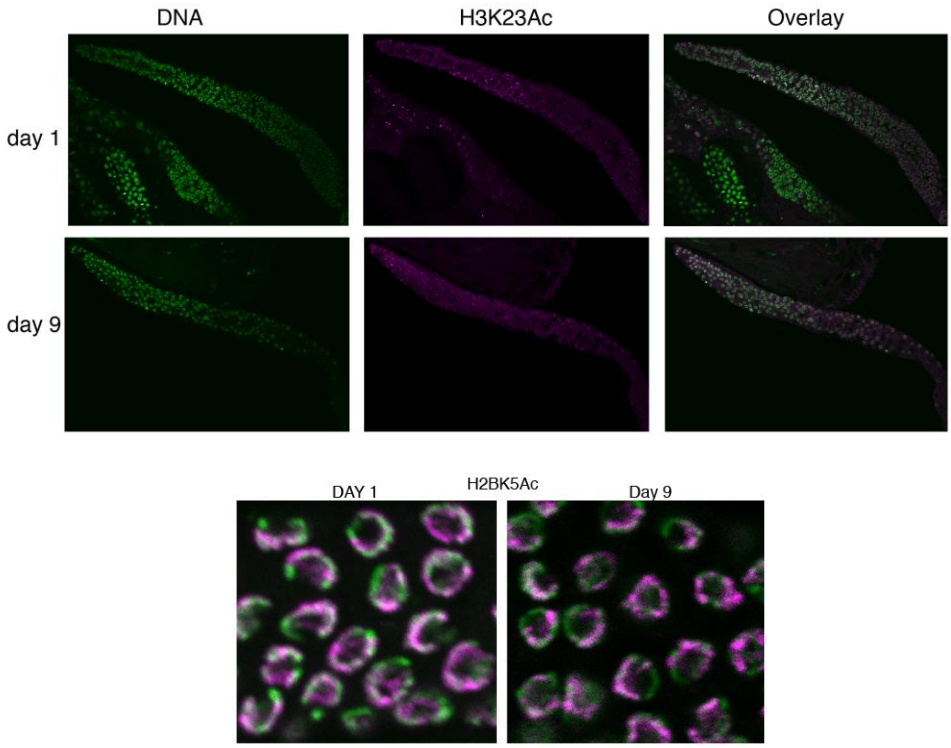

Figure 1. A) Histone H3 Lysine 23 Acetylation (H3K23Ac) and B) histone H2B lysine 5 Acetylation (H2BK5Ac) show no changes in distribution or intensity over the course of reproductive life (DNA, green; histone antibody, magenta).

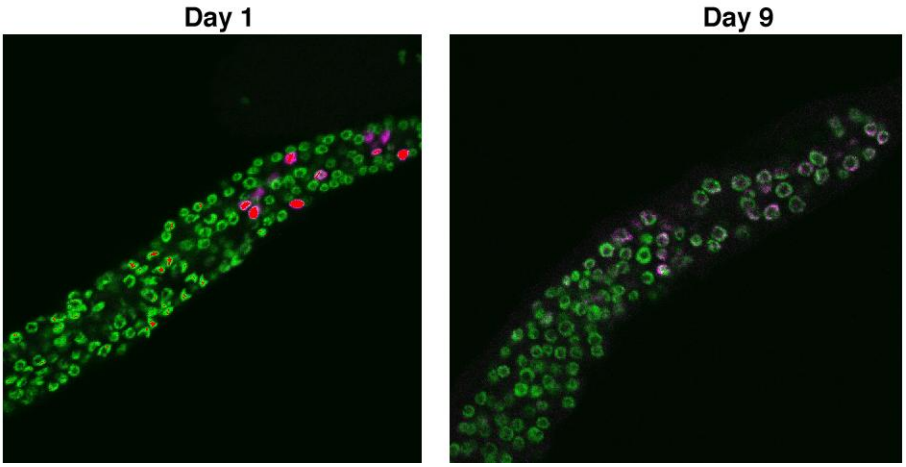

Figure 2. H3Serine10 Phosphorylation is altered in aged germlines. This histone modification is a marker of proliferative and brightly stains cells in mitosis, fading in newly divided cells. In the older germline, the strong staining is absent or rare, but rather all of the nuclei in what is normally the proliferative zone weakly stain for this the presence of this modification.

A.

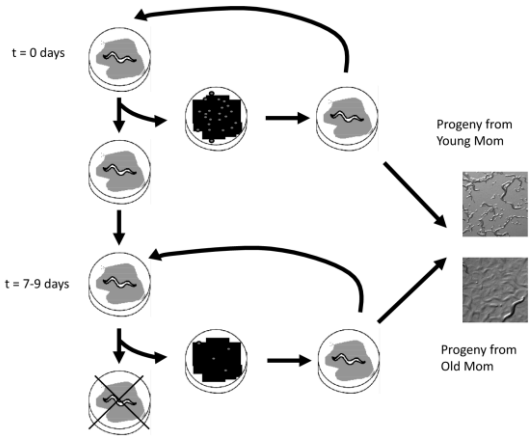

B.

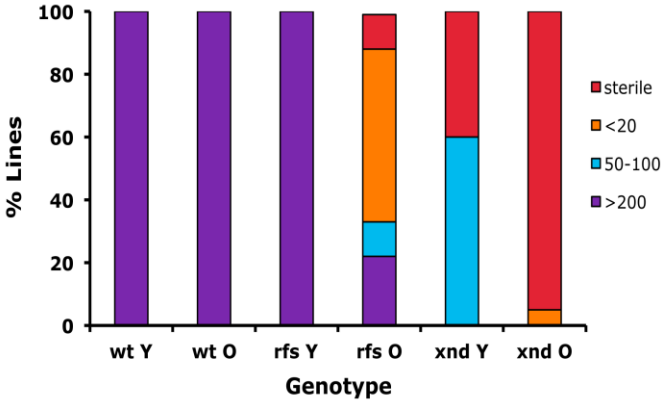

Figure 3. Inbred lines of young and old mothers show reproductive differences. A) Schema for generating inbred lines. The first and last progeny produced from a (mated) mother are iteratively selected. Progeny counts are assessed after *n* generations to determine fecundity. B) No differences in wild type fecundity are observed in five generations of old mothers. In contrast, old mothers mutant for either *rfs-1* or *xnd-1* showed a dramatic decrease in brood size and increase in sterility (wt, wild type; rfs, *rfs-1(ok1372)*; xnd, *xnd-1(ok709)*; Y, young mothers; O, old mothers)